Available online at www.sciencedirect.com
SCIENCE DIRECT®
Ecological Modelling 183 (2005) 323–346
ECOLOGICAL MODELLING
www.elsevier.com/locate/ecolmodel

A bio-physical coastal ecosystem model for assessing environmental effects of marine bivalve aquaculture

Michael Dowd*

Department of Mathematics and Statistics, Dalhousie University Halifax, Nova Scotia, Canada B3H 3J5

Received 30 July 2003; received in revised form 6 April 2004; accepted 9 August 2004

Abstract

A simple lower trophic level, bio-physical marine ecosystem model is developed for the purpose of assessing the environmental effects of bivalve aquaculture in coastal embayments. The ecosystem box model includes pelagic and benthic components and describes the cycling of a most-limiting nutrient. The pelagic compartment is comprised of phytoplankton, zooplankton, nutrients and detritus. These populations interact following predator–prey dynamics and biogeochemical processes. Mixing processes within the bay, and exchange of waters with the adjacent open ocean, are included. The pelagic ecosystem is coupled to a simple benthos containing a dynamically active organic matter pool. Benthic–pelagic coupling includes episodic resuspension, remineralization, sinking, and permanent burial. A population of grazing bivalves is superimposed on this system as a diagnostic variable. The model is applied to a coastal bay and used to determine how bivalve populations affect nutrient cycling in the ecosystem. This is done by examining changes in the standing stock of the various populations, as well as associated nutrient (mass) fluxes, for cases both with and without intensive bivalve culture. It was demonstrated that bivalves divert production from the pelagic to benthic food webs. Phytoplankton and detritus are depleted from the water by bivalve filter feeding and biodeposited to the benthos as fecal matter. This organic loading causes order of magnitude changes in the benthic detrital pool and the associated benthic–pelagic fluxes. It was also shown that water motion and mixing is important in structuring the ecological dynamics in the bay. To faciliate future applications and observational studies, a retrospective analysis of parameter identifiability and uncertainty was also undertaken.

Keywords: Aquaculture; Benthic–pelagic coupling; Nutrient cycling; Box model; Differential equations; Regression

1. Introduction

The global production of marine bivalve aquaculture, including species such as mussels, clams, oysters and scallops, continues to expand (New, 1999). Filter feeding bivalves depend on the coastal marine

* Tel.: +1 902 494 1048; fax: +1 902 494 5130.
E-mail address: Michael.Dowd@Dal.Ca.

0304-3800/$ – see front matter © 2004 Elsevier B.V. All rights reserved.
doi:10.1016/j.ecolmodel.2004.08.018

ecosystem to supply food in the form of suspended particulate matter, both living and detrital. Large bivalve populations can lead to a variety of ecosystem effects. This includes the localized depletion of suspended particulate matter in the vicinity of dense aggregates of bivalves (Incze et al., 1981; Fréchette et al., 1989). It has also been suggested that the grazing activity of bivalve populations controls plankton dynamics on the scale of entire embayments (Cloern, 1982; Dame and Prins, 1998). Alpine and Cloern (1992) conclude that the establishment of large bivalve populations can significantly alter mass and energy flows in coastal ecosystems. Bivalves filter particulate matter suspended in the water column and biodeposit it to the seabed in the form of large and rapidly sinking fecal matter; this diverts production from the pelagic to benthic food webs (Cloern, 1982; Noren et al., 1999). Such high rates of organic biodeposition have been shown to result in anaerobic benthic environments (Hatcher et al., 1994), and change the benthic faunal community (Crawford et al., 2003). Benthic nutrient remineralization may also increase near aquaculture sites due to increased organic matter sedimentation (Grant et al., 1995). Ammonia excretions associated with bivalve culture can influence nutrient levels in seawater in some coastal regions (Dame et al., 1991). Harvesting activities remove biomass directly and Kaspar et al. (1985) suggests that this may contribute to nitrogen limitation in some systems.

Bivalve aquaculture depends on the biological production of the coastal marine ecosystem. Mathematical models are useful for understanding and assessing the potential interactions in these complex manipulated ecosystems. Bio-physical models are required which consider both interacting populations in the coastal marine ecosystem, as well as hydrodynamic influences brought about by water circulation and mixing (Dowd, 2003; Duarte et al., 2003). Ecosystem box models that focus on predicting bivalve growth and carrying capacity have been proposed by Raillard and Ménesguen (1994) and Dowd (1997). Chapelle et al. (2000) also considers an aquaculture ecosystem using a box model approach with an emphasis on the ecosystem effects of land runoff. Both Pastres et al. (2001) and Duarte et al. (2003) present sophisticated ecosystem models fully coupled to hydrodynamic models, and including bivalve bioenergetics. Here, we offer a general, and relatively simple, bio-physical coastal ecosystem model for the purpose of systematically investigating the effects of intensive marine bivalve culture on its supporting ecosystem.

This study outlines the development and application of a simple lower trophic level ecosystem model. The physical situation is one of a shallow, semi-enclosed embayment exchanging its waters (and the freely floating ecosystem components) with the adjacent open ocean. Seasonal time scales are emphasized. The pelagic compartment is comprised of phytoplankon, zooplankton, nutrients and detritus. The pelagic ecosystem is coupled to a very simple, but dynamically active, benthos. A population of grazing bivalves is also included. In Dowd (1997), it was shown that treating the bivalve population as a prognostic variable (i.e. superimposing a bioenergetic model on one of the supporting ecosystem) lead to a degradation in the predictive skill of the model. Since the focus here is not on the prediction of bivalve growth and carrying capacity, bivalve biomass is prescribed and interacts with the ecosystem as a diagnostic variable or forcing function (Kremer and Nixon, 1978; Chapelle et al., 2000). The primary objective of this study is to develop and apply a general mathematical modelling framework for the assessment of ecosystem effects of marine bivalve culture. A secondary emphasis considers how one might analyse the model dynamics in order to identify important parameters, and to determine which variables should be measured in an observational program.

This paper is organized as follows. Section 2 describes the lower trophic level bio-physical ecosystem model including a description of the various pelagic and benthic processes. In Section 3, a specific application of the model is outlined for a semi-enclosed tidal embayment located off eastern Canada. Section 4 presents results from model simulations with an emphasis on how bivalve culture can alter ecosystem fluxes. A retrospective analysis of the model dynamics is also undertaken. A summary and conclusions follows in Section 5.

2. Model

The model describes a simple coastal marine ecosystem with bivalve aquaculture. A conceptual diagram showing the ecological components and their interactions is given in Fig. 1. Population interactions occur within a finite volume of water, or a box. Pelagic ecosystem components include phytoplankton

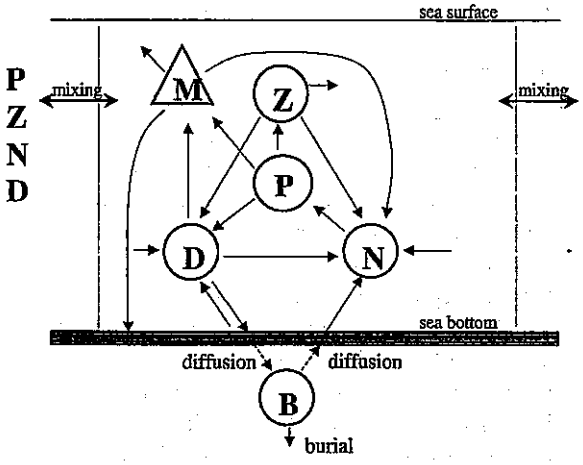

Fig. 1. Conceptual diagram for the ecosystem box model. Prognostic ecosystem state variables are phytoplankton (P), zooplankton (Z), nutrients (N), pelagic detritus (D), and benthic detritus (B). Bivalves, M, are a diagnostic variable. Arrows represent mass, or nutrient, fluxes.

(P), zooplankton (Z), nutrients (N) and detritus (D). These are suspended or dissolved in seawater and are subject to transport through water motion and mixing; by this mechanism they are exchanged with adjacent regions. The benthic compartment contains a detrital organic matter pool (B). A population of spatially fixed grazing bivalves (mussels or M) is superimposed on the system. Note that M is distinguished from the other ecosystem components since its biomass is prescribed at a steady state level. The other ecosystem components are prognostic variables which interact with one another and dynamically co-evolve.

In words, changes in ecological state variables P, Z, N, D and B are given by,

$$\frac{dP}{dt} = +\text{growth} - \text{losses} - Z, M \text{ grazing} \pm \text{mixing}$$

$$\frac{dZ}{dt} = +\text{growth} - \text{losses} \pm \text{mixing}$$

$$\frac{dN}{dt} = +\text{sources} + D, B \text{ remin} + Z, M \text{ excretion} - P \text{ uptake} \pm \text{mixing}$$

$$\frac{dD}{dt} = +\text{sources} - \text{remin} - \text{sed} + P, Z \text{ losses} + B \text{ resusp} - M \text{ grazing} \pm \text{mixing}$$

$$\frac{dB}{dt} = -\text{resusp} - \text{remin} - \text{burial} + D \text{ sed} + M \text{ biodeposition}.$$

Here, $d\{\cdot\}/dt$ represents the time rate of change. Note that mixing acts only on the freely floating pelagic state variables and can either increase or decrease their concentration. Mussels are assumed to be maintained at a constant biomass through harvesting activities. Mussels then participate in material cycling and interact with the ecosystem according to the following

$$\frac{dM}{dt} = 0 = \text{harvest} - (\text{ingestion} - \text{feces} - \text{excretion}).$$

Mathematically, the prognostic ecosystem variables within a box evolve according to the following nonlinear system of ordinary differential equations:

$$\frac{dP}{dt} = f\{N;k_n\}\gamma_p P - \lambda_p P - f\{P;k_p\}I_z Z - I_m P + K(P_\infty - P) \quad (1)$$

$$\frac{dZ}{dt} = \epsilon_z f\{P;k_p\}I_z Z - \lambda_z Z + K(Z_\infty - Z) \quad (2)$$

$$\frac{dN}{dt} = N_{\text{in}} + \phi_d D + \eta^{-1}\phi_b \tilde{B} + \beta_z f\{P;k_p\}I_z Z + \beta_m I_m(P+D) - f\{N;k_n\}\gamma_p P + K(N_\infty - N) \quad (3)$$

$$\frac{dD}{dt} = D_{\text{in}} - \phi_d D - \lambda_d D + \lambda_p P + (1-\epsilon_z-\beta_z) \times f\{P;k_p\}I_z Z + \eta^{-1} r - I_m D + K(D_\infty - D) \quad (4)$$

$$\frac{dB}{dt} = -r - \phi_b \tilde{B} - \alpha \tilde{B} + \eta\lambda_d D + \eta(1-\epsilon_m-\beta_m)I_m(P+D). \quad (5)$$

The steady state assumption for M growth ($dM/dt = 0$) means that the harvest rate is balanced by the net rate of production, both of which are given by $\epsilon_m I_m (P+D)$.

All quantities used in this model are summarized in Table 1. The exception is $\tilde{B}$, which represents a linear transformation of $B(t)$ and is defined in Section 2.3. The nondimensional modulation functions f are of the form

$$f\{X; k_x\} = \frac{X}{k_x + X} \tag{6}$$

where X in the above is one of P or N. The mixing term for the pelagic state variables has been replaced with a gradient-flux relation of the form $K(X - X_\infty)$ and is discussed in Section 2.1. State variables and model parameters are all non-negative; the sign of each term correponds to the direction of mass flow as indicated by the arrows in Fig. 1. Pelagic state variables are in concentration units, while B is measured on a per unit area basis. Cycling of material is defined in terms of a most limiting nutrient which for many temperate marine systems is considered to be nitrogen (Parsons et al., 1977). Ecosystem components are, however, measured in units of carbon equivalents such that 1 g carbon = 10 mmol nitrogen (Steele and Henderson, 1981; Fasham, 1993; Edwards, 2001). The various bio-physical processes in the model are explained in detail below.

Table 1
Definition of quantities in the ecosystem model

Quantity	Units	Value	Definition
(i) State variables			
P	gC m^{-3}	Eq. (1)	Phytoplankton
Z	gC m^{-3}	Eq. (2)	Zooplankton
N	gC m^{-3}	Eq. (3)	Nutrients
D	gC m^{-3}	Eq. (4)	Water column detritus
B	gC m^{-2}	Eq. (5)	Benthic detritus
(ii) Parameters			
K	d^{-1}	Appendix A	Exchange/flushing coefficient
k_n	gC m^{-3}	0.2	Half-saturation for N uptake by P
$\gamma_p(t, \text{Temp})$	d^{-1}	Eq. (8)	P growth rate
λ_p	d^{-1}	0.1	Loss term for P
I_z	d^{-1}	0.5	Ingestion rate for Z on P
k_p	gC m^{-3}	0.1	Half-sat const for Z ingestion of P
ϵ_z	–	0.3	Assim fraction for Z ingested ration
β_z	–	0.4	Excreted fraction for Z ingested ration
λ_z	d^{-1}	0.1	Loss term for Z
$\phi_d(\text{Temp})$	d^{-1}	(0.02–0.1)	Remin rate of D to N
λ_d	d^{-1}	0.05	Sinking rate for D
$\phi_b(\text{Temp})$	d^{-1}	0.01	Remin rate for B to D
$r(t)$	gC m^{-3} d^{-1}	Eq. (9)	Resuspension flux
α	–	0.05	Burial fraction
I_m	d^{-1}	Section 3	Ingestion rate of bivalves
ϵ_m	–	0.1	Assimilated fraction for bivalves
β_m	–	0.1	Excreted fraction for bivalves
η	m	5	Water depth
(iii) External inputs			
$P_\infty(t)$	gC m^{-3}	Fig. 4a	Far-field P
$Z_\infty(t)$	gC m^{-3}	Fig. 4b	Far-field Z
$N_\infty(t)$	gC m^{-3}	Fig. 4c	Far-field N
$D_\infty(t)$	gC m^{-3}	Fig. 4d	Far-field D
$N_{\text{in}}(t)$	gC m^{-3} d^{-1}	Section 3	External N input
$D_{\text{in}}(t)$	gC m^{-3} d^{-1}	Section 3	External D input

Groupings are according to variable type. For each quantity the following information is given: units, its numerical value (or its source), and a brief definition. Explicit functional dependence on time (t) or temperature (Temp) is indicated. Here gC denotes grams carbon, m is metres, and d is days. See text for details.

2.1. Exchange and mixing

The model ecosystem (1)–(5) is considered in the context of a box model. All ecological interactions occur within a finite volume, or box. Components are assumed to be distributed homogeneously within a box, and spatial gradients occur between boxes. Each of the pelagic components of the ecosystem are exchanged with its corresponding population in adjacent areas according to the motion of the fluid in which they are embedded. The horizontal exchange of material is given by

$$\dot{X} = K(X_\infty - X) \tag{7}$$

where $\dot{X} = \mathrm{d}X/\mathrm{d}t$. Here, X represents the concentration the pelagic ecosystem components, i.e. one of P, Z, N, or D. The corresponding value in the adjacent box is X_∞. The parameter K is an exchange coefficient that scales the concentration difference between the regions. Eq. (7) describes a gradient-flux relation consistent with Fickian diffusion (Fischer et al., 1979). The parameter K includes a variety of physical processes, such as tidal mixing, and can be interpreted as an inverse time scale for the flushing of the box. A term of the form (7) is appended to each of (1)–(4) to represent mixing processes. Multiple boxes can be combined to

add a spatial aspect to the time dependent ecosystem model.

An illustrative example of the use of (7), which anticipates the application in Section 3, is the following. Consider a shallow, semi-enclosed embayment which is well mixed in the vertical and horizontal, and thereby can be considered as a box. The far-field concentrations of the ecosystem components in the adjacent open ocean are X_∞. Their time-varying level might be specifed as a type of boundary condition, or forcing function. Ecological interactions described by (1)–(5) occur within the bay, and pelagic ecosystem components are exchanged between the ocean and the bay. A key element of the box model is the control of the internal ecosystem processes by the far-field conditions, which brings about a form of ecosystem closure. The addition of mixing terms has been shown to lend stability to an ecosystem (Edwards et al., 2000; Edwards, 2001). In more general ecological terms, it is an example of an open system which allows components to disperse, or exchange, outside the control volume (Nisbet et al., 1997).

2.2. Pelagic processes

The pelagic part of the model includes the biotic components, P and Z, and the abiotic components, N and D. These are found in the water column as suspended (P, Z, D) or dissolved (N) material. Consider the pelagic ecosystem equations (1)–(4), ignoring the terms related to benthic–pelagic coupling ($r = \phi_b = 0$). Also suppose that no bivalves are present ($I_m = 0$). The model (1)–(4) then reduces to a basic form of the widely used *PZND* model. This generalized predator–prey model has its roots in the classic study of Riley (1947) and a *PZN* model was originally used to describe plankton dynamics in the oceanic mixed layer (Steele and Henderson, 1981; Evans and Parslow, 1985). Fasham et al. (1990) added a detrital component to account for organic matter breakdown by marine bacteria, or the so-called microbial loop. Such *PZND* models are now being widely applied in biological oceanography (Kemp et al., 2001; Waniek, 2003). Because of the complex dynamical properties inherent in even the most simple *PZND* models (Franks et al., 1986; Edwards, 2001), as well as our goal of a general understanding of aquaculture effects on the cycling of matter in shallow coastal marine ecosystems, a simple form of the *PZND* model is used. The pelagic processes considered here include: (i) primary production, (ii) predation, and (iii) biogeochemistry. These are discussed below.

2.2.1. Primary production

Phytoplankton growth is governed by the seasonally varying maximum light limited photosynthetic rate γ_p. It is computed as a daily and depth averaged growth rate according to

$$\gamma_p(t, \text{Temp}) = \frac{chl}{C}\frac{1}{\eta T}\int_0^T \int_0^\eta g\{I(z,t);\theta(\text{Temp})\} \times \mathrm{d}z\,\mathrm{d}t \quad (8)$$

where T here corresponds to one day, η is the depth of the water column, and chl/C is the chlorophyll-a to carbon ratio of the phytoplankton. The photosynthesis–irradiance curve is given by $g\{\cdot\}$ and uses the functional form reported in Platt et al. (1980). It is a function of the seasonally and diurnally varying underwater light field $I(z, t)$. The photosynthetic parameters θ are taken from Platt and Jassby (1976) and modified using the temperature modulation of Epply (1972).

The growth rate γ_p in (1) is reduced by nutrient limitation imposed by the saturation function $f\{N; k_n\}$. This is interpreted here in the context of Michaelis-Menten kinetics (Caperon, 1967; Dugdale, 1967). This autotrophic process results in the uptake of inorganic N and its conversion to organic P. Phytoplankton losses occur through mortality at a constant rate λ_p and directly enter the detrital pool; its numerical value in Table 1 is taken from Le Pape et al. (1999). Note that we do not consider self-shading in these shallow coastal systems where light attenutation is controlled mainly by non-plankton suspended particulate matter.

2.2.2. Secondary production

Secondary production includes zooplankton and bivalve growth. Zooplankton consume phytoplankton according to the ingestion function $f\{P; k_p\}$ which here describes a Holling type II functional response where the predator's ingestion of prey saturates with increasing prey density (Holling, 1959). This process is well established for Z grazing on P (Frost, 1975). The ingested ration is partitioned into three components: (i) a fraction ϵ_z incorporated into biomass growth, (ii) a

fraction β_z excreted into the N pool, and (iii) the remaining fraction, $1 - \epsilon_z - \beta_z$, lost through fecal production to D. A constant loss rate λ_z governs natural mortality and higher order predation on Z. Numerical values for these parameters in Table 1 follows Edwards (2001) and references therein.

Bivalves are treated as a diagnostic variable which affect the ecosystem through the processes of ingestion, excretion and fecal production. Their population dynamics is mainly under the control of aquaculturalists through stocking and harvesting activities and a steady state assumption has been made for their biomass, i.e. the instantaneous M production rate $\epsilon_m I_m(P + D)$ is assumed to be exactly equal to the removal rate through harvesting. Filter feeding bivalves consume both P and D. The ingestion rate I_m is based on their volumetric clearance of particulates in a water mass, a process consistent with a type I functional response (Hassell, 1978). Knowledge of the clearance rate (measured in units of $m^3\,d^{-1}\,kg^{-1}$) and the M biomass density ($kg\,m^{-3}$) allows computation of the ingestion rate I_m (d^{-1}). Following Z above, the total ingested ration $I_m(P + D)$ is partitioned into three components for growth, excretion and feces, as dictated by the parameters ϵ_m and β_m. The fraction $1 - \epsilon_m - \beta_m$ is comprised of mussel feces and pseudofeces and, unlike Z, these particle aggregates sink rapidly and are biodeposited directly into the benthic detrital pool B (Widdows et al., 1998). The growth rate of M is constrained to balance the harvest rate so that total M biomass remains constant. Values for ϵ_m and β_m in Table 1 are taken from Griffiths and Griffiths (1987).

2.2.3. Pelagic biogeochemistry

Particulate organic matter, D, suspended in the water column receives inputs from the mortality of both P and Z. Breakdown of organic D to inorganic nutrients, N, by marine bacteria takes place on a time scale of days (Heip et al., 1995). This remineralization process occurs at a rate ϕ_d which is proportional to the level of D. Jones and Henderson (1986) report a range for ϕ_d of 0.004–0.18 d^{-1}. Here, a temperature dependent remineralization rate of the form $\phi_d = \text{const} \times \exp(Q(\text{Temp} - \overline{\text{Temp}}))$ is used with the coefficients determined so as to fall into this reported range. Water column detrital matter is also exchanged with the benthos through sinking and resuspension as discussed in Section 2.3.

The nutrient pool, N, receives the remineralized D. It also receives the excretion products from Z and M, as fractions (β_z, β_m) of their ingested ration. The main N sink in the water column is its uptake by P as dictated by primary production. The benthos also provides an N source through remineralization of benthic detrital organic matter, B, and is discussed below.

2.3. Benthic processes

The time evolution of the benthic detrital pool, B, is given by (5). In shallow coastal ecosystems there is a strong interaction between the water column and the benthos. Here, a simple benthos is coupled to the pelagic model to account for the major bio-physical processes which affect the water column. This viewpoint avoids detailed biogeochemical and sediment transport models in favor of a very simple description of their emergent properties.

Note that in the model (1)–(5) the pelagic components P, Z, N, and D are measured on a per unit volume basis as concentrations ($gC\,m^{-3}$), whereas B is measured as mass per unit area ($gC\,m^{-2}$). The mass fluxes associated with benthic–pelagic coupling must be modified accordingly: a flux from a pelagic component to B is multiplied by the water depth η, while fluxes from B to the pelagic components are divided by η.

2.3.1. Sinking, resuspension and burial

The net input flux of detritus from the water column to the benthos is governed by sedimentation and resuspension. Sinking of detrital matter represents a flux from D to B. The sinking rate of suspended particles, or particle aggregates, is affected by both water turbulence as well as particle characteristics, such as their density and size. The representation of sinking in (4) and (5) assumes it is proportional to D and occurs at a constant rate λ_d. Setting $\lambda_d = 0.05\,d^{-1}$, $D = 1\,gC\,m^{-3}$ and $\eta = 5$ m depth translates to an annual flux $\eta\lambda_d D$ to the benthos of near 100 $gC\,m^{-2}\,year^{-1}$. This is consistent with the coastal sedimentation rates compiled by Heip et al. (1995).

Resuspension represents a detrital flux into the water column, D, from the benthos, B. Physically, this flux is driven by the exceedance of a critical bottom shear stress, or near-bed erosional velocity, which can set particles in motion and entrain them into the overlying

fluid. This process depends on large and small scale water motions in the benthic boundary layer, as well as on seabed characteristics. It can be considered independent of either D or B (except for the constraint that B must remain non-negative). Resuspension in shallow systems is often forced by wind driven currents and waves. These irregular events occur on short time scales (<1 d), and take the form of large fluxes which disrupt the equilibrium sediment distribution. Resuspension is therefore considered as an idealized event based process, i.e.

$$r(t) = \sum_i c\,\delta(t - t_i) \tag{9}$$

where δ is the Dirac delta function, t_i represents the time of a resuspension event, and c is the event intensity. The flux $\int r(t)\,dt$ over single event cannot exceed the amount of material in B. Here, it is assumed that the time between events, Δt_i, is random and distributed according to an exponential distribution with a seasonally varying width parameter. This mimics wind driven resuspension, with Δt_i ranging from 10 days in the summer to 4 days in the winter consistent with the event frequency in meteorological band from our region, and with the observations reported in Edelvang et al. (2002). The stochastic process described here resembles shot noise in electronic systems and has been extensively analysed in this context (e.g. Gardiner, 1997, Section 1.4).

2.3.2. Benthic remineralization

Mineralization of the benthic detrital pool, B, returns nutrients, N, to the water column. Sediment pore water containing particulate organic matter deposited on the sea floor is transported into the sediment matrix through advective and diffusive processes. This detrital organic matter then undergoes a sequence of biogeochemical reactions in the sediment whereupon remineralized products are released as a diffusive flux into the water column. Diagenetic models are vertically resolved sediment biogeochemical models concerned with a detailed accounting of these processes (Boudreau, 1997). Soetaert et al. (2000) reviews a sequence of approximations to these complex models to facilitate the incorporation of benthic–pelagic coupling in oceanic biogeochemical models.

Here, it is assumed that benthic organic matter decomposes at a rate directly proportional to its own concentration. This follows the widely used one-G biogeochemical model, originally due to Berner (1964), and corresponds to the level 3 model of Soetaert et al. (2000). However, this representation is modified here to better account for higher order effects. Specifically, the N efflux in (5) is given as $\phi_b \tilde{B}$ where

$$\tilde{B}(t) = \int_0^t B(t - \tau)\kappa(\tau)\,d\tau. \tag{10}$$

The quantity $\tilde{B}(t)$ is a convolution of $B(t)$ with the kernel κ. In this study, we use a Gaussian kernel of the form $\kappa(\tau) = \exp(-\tau^2/\zeta^2)/\int_0^t \exp(-\tau^2/\zeta^2)\,d\tau$. Here, ζ has a mean of 20 days but varies smoothly from 10 to 30 days in phase with the temperature. The convolution integral in (10) acts to time shift and smooth $B(t)$, making the N efflux a function of the time history of the input D influx. It is then less dependent on the episodic fluctuations imparted by the δ-forcing in $r(t)$. The temperature dependence of ζ means that the biogeochemistry responds rapidly for small ζ (high temperature), and slowly for large ζ (low temperature). The representation here provides an empirical accounting of the emergent effects of the reaction–diffusion processes which both transport and transform particulate organic matter within the sediments. The remineralized efflux is a smoothed and time shifted version of the depositional influx, as is found in the fully coupled diagenetic model of Soetaert et al. (2000, Fig. 3c). A similar rationale applies to the burial process in (5), wherein a small fraction of the organic material $\alpha\tilde{B}$ escapes remineralization and enters the refractory part of the benthic detrital pool to be permanently buried in the sediment (Middleburg et al., 1997). Note that use of $\tilde{B}$ renders the system (1)–(5) non-Markovian, however convolution can be efficiently implemeted using the fast Fourier transform (Press et al., 1996, Chapter 12).

3. Application

The ecosystem box model (1)–(5) was applied to Tracadie Bay, located on Prince Edward Island off the east coast of Canada (Fig. 2). This is a shallow (<7 m) nearly-enclosed tidal embayment (Fig. 3). Oceanographic overviews are given in Dowd et al. (2001, 2002). Currents are both tidal and wind driven. The tidal regime is comprised of mixed diurnal and semidi-

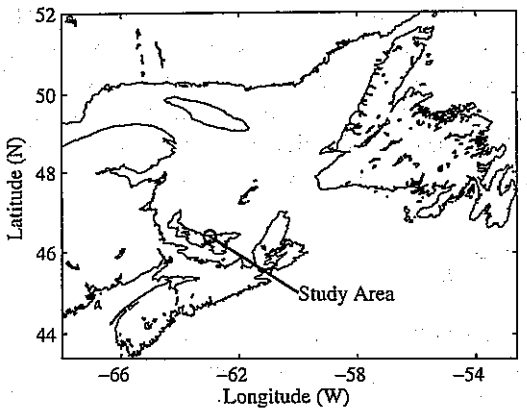

Fig. 2. Location map for the study area.

urnal tides, with a range <1 m. Instantaneous exchange of bay waters with the adjacent Gulf of St. Lawrence is up to 500 $m^3 s^{-1}$. Freshwater inputs are small, with climatological summer values <1 $m^3 s^{-1}$ (Gregory et al., 1993). Tracadie Bay supports extensive bivalve aquaculture in the form of long-line culture of the blue mussel *Mytilus edulis*. There is ongoing concern that the bay has reached its carrying capacity for mussel culture (Page et al., 1999). There is also speculation on possibles changes in nutrient cycling in the ecosystem, as well as shifts in community structure, resulting from intensive bivalve aquaculture (Cranford et al., 2002). Dowd (2003) calculates that in Tracadie Bay the characteristic time scale for: (i) residence time of the water in the bay, (ii) the filtration time for the bivalve population to clear this water, and (iii) the production timescale for the primary producers, are all around 5 days. This implies that water transport processes, internal biological production within the bay, and bivalve grazing activity all play comparable roles in controlling in the cycling of matter in the ecosystem of the bay.

Tracadie Bay was divided into three boxes as shown in Fig. 3. The boundaries were based on circulation and water properties of the bay as reported in Dowd et al. (2001, 2002). The implication is that the regions have distinct and relatively homogenous water properties and gradients occur roughly on the boundaries. The inner regions (boxes 2 and 3) exchange their waters with the open ocean through the central bay (box 1); there is little direct exchange between boxes 2 and 3. Generalizing the relation in (7) and using the ecosystem

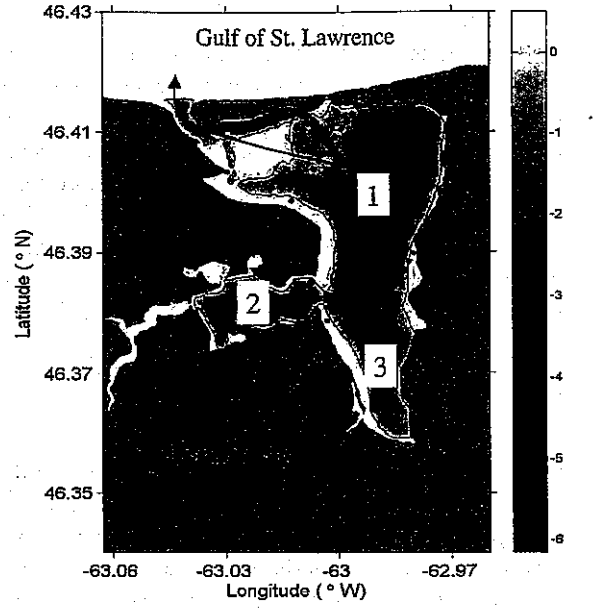

Fig. 3. Map of Tracadie Bay including the bathymetry in grayscale and the contour associated with the intertidal zone (depth in metres). The three boxes and their boundaries are given. Arrows indicate mixing between the boxes, and with the adjacent open ocean.

model (1)–(5) yields a three box system of the form,

$$\dot{X}_1 = h\{[X_1, B_1]'\} + \nu_1 + K_{\infty}(X_{\infty} - X_1) - K_{12}(X_1 - X_2) - K_{13}(X_1 - X_3) \quad (11)$$

$$\dot{X}_2 = h\{[X_2, B_2]'\} + \nu_2 + K_{12}(X_1 - X_2) \quad (12)$$

$$\dot{X}_3 = h\{[X_3, B_3]'\} + \nu_3 + K_{13}(X_1 - X_3). \quad (13)$$

Here, the $X_i = (P_i, Z_i, N_i, D_i)'$ is a vector containing concentrations of the pelagic state variables in box i. The superscript $'$ denotes matrix transpose. The vector function h contains the homogenous terms in the ecosystem dynamics (1)–(5). This operator acts on the full ecosystem state, both pelagic and benthic, for each box. The state independent vector ν_i contains the nonhomogeous terms of (1)–(5), such as N_{in} and D_{in}, for box i. There are three exchange coefficients: K_{∞} represents mixing between the ocean and box 1; K_{12} represents mixing between box 1 and box 2; and K_{13} represents mixing between boxes 1 and 3.

Numerical values are required for the three exchange coefficients. These were determined by inversion of a heat budget model using observed temperature time series for each of the boxes. Details are given in

Appendix A. The following estimates for the exchange coefficients were obtained: $K_{\infty} = 1.3$, $K_{12} = 0.4$ and $K_{13} = 0.5$ in units d^{-1}. The expected time for the material to remain in each of three boxes are 0.6, 2.5 and 2.2 days, respectively. For 90% of the material to removed, the corresponding timescales are 1.2, 7.6 and 6.4 days. The interested reader is referred to Takeoka (1984) for more details on computing residence times.

The general mathematical structure for the ecosystem dynamics was described in Section 2. Application of this model to a specific situation, such as that of Tracadie Bay, requires a number of quantities be specified. These include: initial conditions for each of the state variables; numerical values for the model parameters; internal source or sink terms; and far-field values of the pelagic state variables. Time integration of the model produces predictions for each of the state variables. The rationalization for model parameter values was given in Section 2 and numerical values are found in Table 1. Specification of the remaining model inputs is outlined below.

Idealized annual cycles for each of the far-field pelagic state variables are given in Fig. 4. These external source terms correspond to concentrations of the pelagic state variables in the adjacent Gulf of St. Lawrence. They were obtained as follows.

- $P_{\infty}(t)$: The annual cycle of chlorophyll concentration from the region adjacent to Tracadie Bay was determined from biweekly composite SeaWIFS satellite images compiled at the Bedford Institute of Oceanography. These were converted to carbon units by assuming a carbon:chlorophyll-a ratio of 50:1.
- $Z_{\infty}(t)$: Zooplankton are assumed to be a reduced magnitude, smoothed and lagged version of the phytoplankton time series. This assumption is consistent with observed Gulf of St. Lawrence copepod biomass (Fisheries & Oceans Canada, Atlantic Zonal Monitoring Program).
- $N_{\infty}(t)$: A compilation of nitrate and ammonium from the adjacent Gulf of St. Lawrence yielded mean winter values near 5 mmole $N\,m^{-3}$ (or $0.5\,gC\,m^{-3}$) and summer values near 1 mmole $N\,m^{-3}$ ($0.1\,gC\,m^{-3}$), but with a high degree of scatter (Dr. Peter Strain, Bedford Institute of Oceanography, personal communication). These values motivate the idealized seasonal nutrient cycle.
- $D_{\infty}(t)$: Detritus was simply assumed to be constant with a level of $0.6\,gC\,m^{-3}$. Time series of point measurements made in and near Tracadie Bay exhibited high variability and an apparent lack of a seasonal

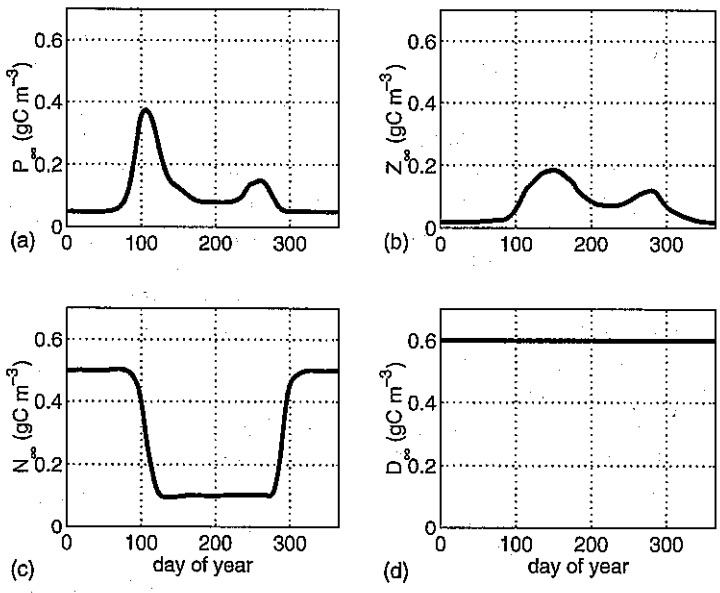

Fig. 4. Annual cycle of the far-field concentrations of the pelagic state variables P_{∞}, Z_{∞}, N_{∞} and D_{∞}. The time axis covers the calendar year.

cycle. A representative annual mean value was chosen.

The temperature cycle is also required for its role in modulating the remineralization rates, as well as the phytoplankton growth rate. A sine curve was fit to the annual cycle of observed temperature yielding $\text{Temp}(t) = 10 + 11\sin(\omega t + 4\pi/3)$, where t is in days, $\omega = 2\pi/365$ and $\text{Temp}(t)$ is in degrees Celsius.

Internal source terms, N_{in}, for nutrients were considered to be non-zero only for box 2, which receives the bulk of the nutrient inputs from land-based sources via the only substantial freshwater source, Winter River. Nitrogen values measured near Winter River in July 1999 were near 30 mmole N m^{-3} (or 3 gC m^{-3}). Gregory et al. (1993) reports a mean freshwater flux of 1 $\text{m}^3\ \text{s}^{-1}$ for Tracadie Bay. Assuming this input N flux is uniformly distributed over box 2, which has a volume near $10^7\ \text{m}^3$, yields a input flux of 0.025 gC $\text{m}^{-3}\ \text{d}^{-1}$. A detrital input term, D_{in} was also included in (4), and in Tracadie Bay results from land-runoff and the decay of macrophyte detritus. A value of 0.03 gC $\text{m}^{-3}\ \text{d}^{-1}$ was assumed for all boxes. This allows interior values of D to match far-field values D_∞, consistent with the relative lack of spatial gradients in detritus as reported in Dowd (2003).

The phytoplankton growth rate γ_p was computed according to (8). A carbon to chlorophyll ratio of 50 was assumed. Surface solar irradiance observations from the region were used along with astronomical relations. The underwater irradiance field was computed using an optical depth of 3m, as measured in various locations during summer 1999. The resultant time series of γ_p is shown in Fig. 5. It is maximal in late August, when light levels are high and water temperatures are relatively warm; a doubling time for phytoplankton of 1 day can be achieved during this period if sufficient nutrients are available.

To apply the model to the present situation in Tracadie Bay, the mussel grazing rate, I_m, must be specified. Government and industy communications lead us to estimate production of mussel biomass in Tracadie Bay at 3×10^6 kg wet weight and the standing stock of mussels at 2×10^6 kg wet weight. Biomass is assumed to be uniformly distributed throughout the bay. I_m is determined as follows. Carver and Mallet (1990) report 80 mussels per kg wet weight in longline culture in the region. Assume also a mean filtration rate of 1 L

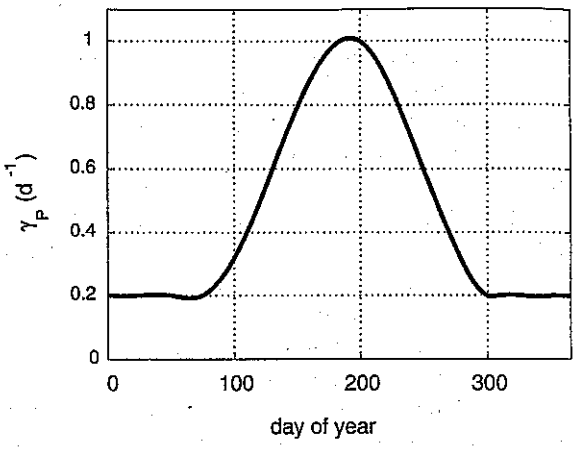

Fig. 5. Annual cycle of the maximum light limited phytoplankton growth rate γ_p. The time axis covers the calendar year.

per individual mussel per hour (Griffiths and Griffiths, 1987). These figures, together with the estimated standing stock and the volume of the bay ($36 \times 10^6\ \text{m}^3$), yields an estimate for I_m near 0.1 d^{-1}.

Numerical implementation of the ecosystem box model proceeds as follows. The governing Eqs. (1)–(5) were discretized and solved using an Euler method (Boyce and DiPrima, 1986, Section 8.2). The system is Markovian except for the convolution in (10) which is associated with benthic remineralization; this term is evaluated every time step and requires past values of the model state. The time step of the model was 0.1 d and the simulation starts at the beginning of the calendar year. Initial conditions for the pelagic state variables P, Z, N, and D are set based on their corresponding far-field values in Fig. 4. This is reasonable for winter periods when the internal ecology in the bay is inactive and the system is controlled by the far-field conditions; pelagic variables equilibrate with the far-field conditions on a time-scale set by the mixing processes (days to weeks). The benthic detrital pool B has a much longer response timescale (months) due to storage effects and remineralization processes. The initial condition for B is a zero field, and the model is integrated for three years until a seasonally varying periodic steady state for B is reached. Model variables are then recorded for one calendar year (January 1 to December 31).

In more general terms, the numerical version of the ecosystem model can be represented by following dis-

crete equation

$$X = f\{\theta\} \tag{14}$$

where X is a $q \times 1$ vector and $q = nmT$. Hence, X contains the $n = 5$ ecosystem state variables for the $m = 3$ boxes and for all model time steps T. Here, the $q \times 1$ vector function f represents the discretized model dynamics. It is a function of the $p \times 1$ vector of model parameters θ which includes all quantities which must be specified to carry out a model run, including the time dependent forcing functions. The model output is a deterministic function of the parameters as dictated by the mapping described by f. To isolate a particular state variable in a particular box denote $X^{(a,b)}$ as the subset of X containing the time series for the ecosystem state variable a located in box b. For example, $X^{1,2}$ would represents ecosystem component 1 (i.e. P) in box 2. This $T \times 1$ vector is determined as $X^{(a,b)} = H^{(a,b)}X$, where $H^{(a,b)}$ is a sparse $T \times q$ matrix which picks out the appropriate elements of X. This is used for model analysis in the next section.

4. Results

4.1. Ecosystem simulations

Model simulations are concerned with predicting the ecosystem effects of intensive bivalve culture. Two cases are considered. These are set up following Sections 2 and 3, and differ only in the level of mussel grazing I_m. (i) Case 1: $M = 0$. This simulation is of a culture free system with no mussels and $I_m = 0$. (ii) Case 2: $M \neq 0$. This simulation take place under the present level of aquaculture activity corresponding to $I_m = 0.1\,\mathrm{d}^{-1}$. The two cases are contrasted to investigate how intensive bivalve culture changes the standing stock of the ecosystem state variables, as well as how it affects mass flows within the ecosystem.

Results from a model simulation for the $M = 0$ case are given in Fig. 6. This shows predicted time series for the pelagic state variables P, Z, N and D for the three boxes in Tracadie Bay. Physical control of pelagic state variables is evident with the standing stock reflecting the corresponding far-field values, particularly the outer bay (box 1). The innermost areas (boxes 2 and 3) deviate more from their far-field values due to weaker coupling with the far-field and the relatively greater importance of internal ecosystem dynamics. The Z follow closely the far-field Z_∞ for all boxes. The D time series exhibits irregular fluctuations as a result of episodic resuspension events, followed by slower exponential settling. The mean level of D is close to the time-invariant D_∞. The dynamics of P indicate an enhanced but near synchronous spring bloom relative to P_∞. This results from high N levels coupled with a high growth potential γ_p. After the bloom, P levels fall. However, through the summer and fall P is enhanced by a factor of 2 to 4 relative to P_∞ due to the high γ_p. Eventually, P declines with low light levels and temperatures. On short time scales, irregularities in N and P are associated with resuspension of detritus, its subsequent remineralization to N, and eventual uptake by P. In box 2, enhanced N and P occur due to riverine nutrient inputs, N_{in}. Remineralization of D increases N levels elsewhere. Summer N levels are controlled largely by P uptake and exchange processes. The winter period effectively resets all the pelagic state variables to their far-field values, with exchange processes dominating over the relatively inactive biological processes.

Fig. 7 shows predicted time series of the pelagic state variables for the case for which mussels were present ($M \neq 0$). (Model predicted mussel harvest, whose computation was outlined in Section 2, was close to independent estimates, thereby providing a consistency check for the mussel mass balance parameters.) In comparison with the $M = 0$ case, the following patterns are evident. D levels are depleted relative to D_∞. This effect is most pronouced in the inner bay and results from the filter feeding mussels removing particulates at a rate faster than they can be renewed by water mixing. Ingested P and D are biodeposited to B leading to an elevated benthic detrital pool. This drives enhanced resuspension and greater variability in the water column D. It also leads to increased levels of N through greater B remineralization. However, in spite of the elevated N, phytoplankton standing stock actually decreases with any new production being rapidly grazed down by M. The corresponding Z levels are also lower due to depletion of their food source.

Time series of the benthic detrital pool, B, are shown in Fig. 8 for both the $M = 0$ and $M \neq 0$ cases. Within each case, there is relatively little difference between the boxes and the figure reports only the time-varying

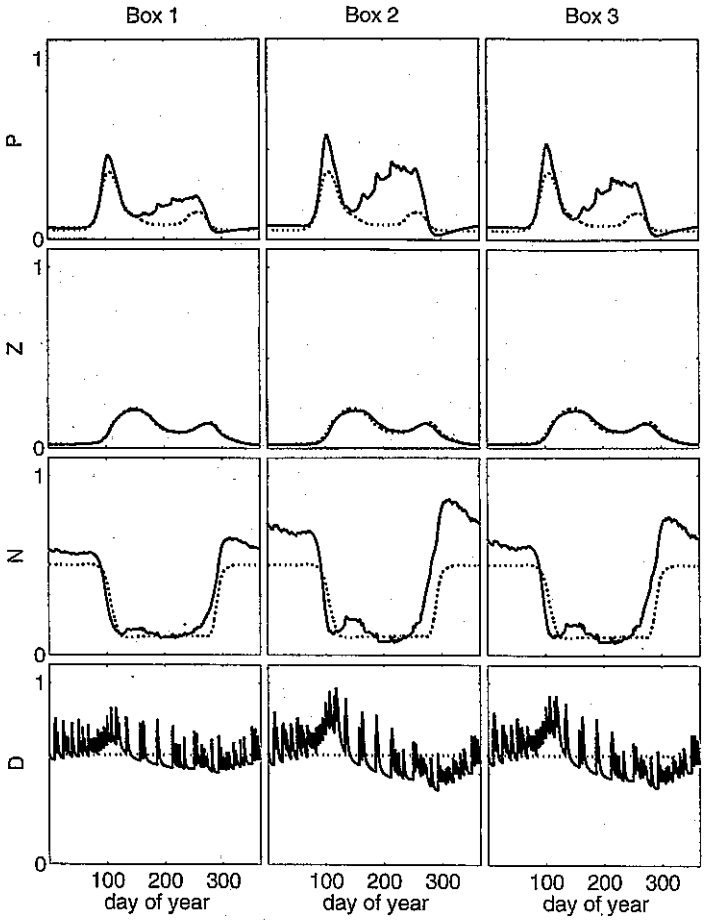

Fig. 6. Simulated time series of the pelagic state variables for the $M = 0$ case. Columns correspond to three boxes. Rows correspond to state variables. Solid lines refer to P, Z, N and D in the box, while dotted lines are the reference far-field (P_∞, Z_∞, N_∞, D_∞). The time axis covers the calendar year.

mean of B over all three boxes. The B time series is dominated by high frequency fluctuations associated with resuspension and settling, but also influenced by the processes of benthic remineralization and burial. The benthic detrital pool is an order of magnitude larger for the $M \neq 0$ case, as compared to the $M = 0$ case. For the case $M = 0$, little permanent detrital accumulation is evident, only temporary storage of B which is frequently resuspended. For the $M \neq 0$ case, mussel biodeposition leads to accumulation of up to 7 gC m^{-2}, with the low frequency portion of B reaching a quasi-periodic steady state for its annual cycle. The seasonal cycle in B shows a rapid increase following the spring phytoplankton bloom, after which a steady decay occurs as sediment biogeochemistry becomes active with increasing summer temperatures.

Table 2 shows the annual fluxes for all the ecosystem components for both the $M = 0$ and $M \neq 0$ cases. These are reported as areal measures (in gC m^{-2} $year^{-1}$) to allow direct comparison of the benthic and pelagic components. (Note that each of these mass fluxes corresponds to one of the arrows in Fig. 1). Fluxes between the pelagic components for the $M = 0$ case are dominated by nutrient uptake associated with primary production ($N \rightarrow P$), and water column remineralization ($D \rightarrow N$). With $M \neq 0$ significant amounts of D are also removed from the water column by bivalve filter feeding ($D \rightarrow M$), an effect

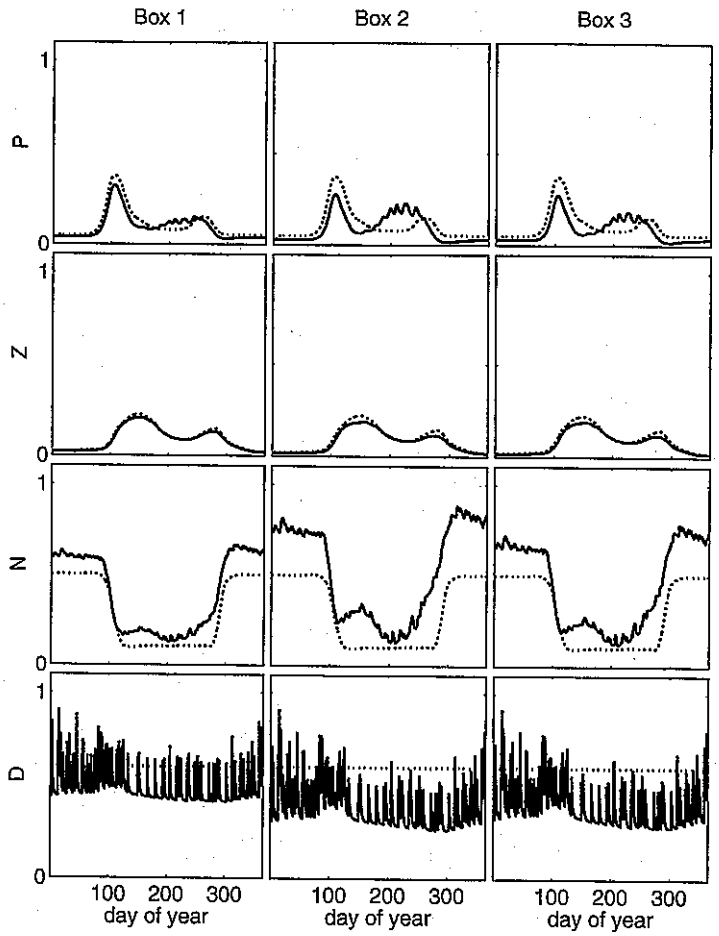

Fig. 7. Simulated time series of the pelagic state variables for the $M \neq 0$ case. Columns correspond to three boxes. Rows correspond to state variables. Solid lines refer to P, Z, N and D in the box, while dotted lines are the reference far-field (P_∞, Z_∞, N_∞, D_∞). The time axis covers the calendar year.

which is most pronounced in the inner boxes. Benthic–pelagic fluxes in the $M = 0$ case are such that sedimentation slightly exceeds resuspension with most of the difference being buried. With $M \neq 0$, biodeposition of mussel feces ($M \rightarrow B$) dominates the organic matter flux to the benthos. As a consequence the B pool increases, and order of magnitude changes are seen in benthic remineralization ($B \rightarrow N$) and burial. The resuspension flux is also doubled. These effects are similar between boxes. Hargrave (1985) reports natural sedimentation rates of 0.1 to 1 gC m^{-2} d^{-1}. By summing the $D \rightarrow B$ and $M \rightarrow B$ fluxes, it is seen that the $M = 0$ case falls at the lower end of this range, while the $M \neq 0$ case falls at the mid to upper end of the range. Examination of the source and sink terms indicate that with an increased bivalve population the system becomes a strong importer of P and D, and an exporter of N. The flux of Z to higher trophic levels seems little affected by M levels.

4.2. Model analysis

In order to facilitate further application of the ecosystem model, an analysis of some of its dynamical properties was undertaken. These were assessed in order to better understand model structure, and to help

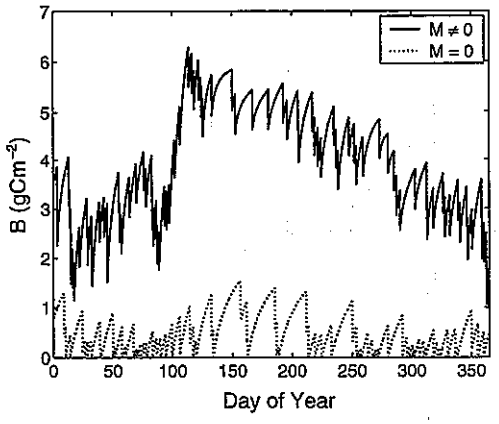

Fig. 8. Time series for the benthic detrital pool B for the two cases with ($M \neq 0$) and without ($M = 0$) mussels present. The values of B shown in each case are averages over all three boxes. The time axis covers the calendar year.

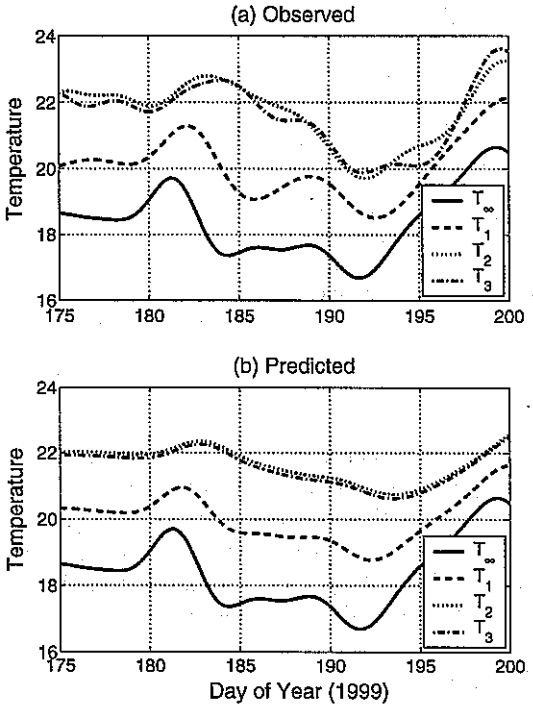

Fig. 9. Observed and predicted temperature records for summer 1999 for the three boxes. Observations were low pass filtered with 100 h cutoff. Predicted temperature is based on the inverse method using the heat equation.

Table 2
Annual fluxes in the ecosystem model in gC m^{-2} $year^{-1}$

Flux	Box 1		Box 2		Box 3	
	$M=0$	$M\neq 0$	$M=0$	$M\neq 0$	$M=0$	$M\neq 0$
(i) Pelagic fluxes						
$N \to P$	72.1	55.2	104.0	65.7	83.3	54.1
$P \to Z$	38.3	30.7	42.3	27.8	39.3	26.5
$P \to D$	20.7	13.6	28.9	13.2	24.6	12.0
$Z \to N$	15.3	12.3	16.9	11.1	15.7	10.6
$Z \to D$	11.5	9.2	12.7	8.3	11.8	8.0
$D \to N$	90.1	73.5	88.2	57.4	87.3	58.9
$P \to M$	0.0	27.3	0.0	26.4	0.0	23.9
$D \to M$	0.0	141.6	0.0	114.3	0.0	117.1
$M \to N$	0.0	16.9	0.0	14.1	0.0	14.1
(ii) Benthic fluxes						
$M \to B$	0.0	135.1	0.0	112.6	0.0	112.9
$D \to B$	43.4	35.4	43.5	28.6	43.1	29.3
$B \to N$	1.9	17.3	1.8	12.2	1.8	12.4
$B \to D$	32.9	67.2	33.0	67.2	32.7	67.2
Burial	8.9	88.5	9.0	63.9	8.8	64.8
(iii) Sources and sinks						
P export	13.1	−16.4	32.8	−1.7	19.4	−8.3
Z export	−1.6	−3.3	−0.3	−3.4	−1.1	−3.8
N export	35.1	64.6	46.6	72.5	21.5	41.6
D export	−9.9	−102.0	71.5	−54.5	−2.7	−61.1
N input	0.0	0.0	43.8	43.8	0.0	0.0
D input	58.4	58.4	58.4	58.4	58.4	58.4
Z output	13.1	12.5	13.0	11.7	12.9	11.8
M output	0.0	16.9	0.0	14.1	0.0	14.1

These are reported for both the $M = 0$ and $M \neq 0$ cases for all three boxes. The notation $X \to Y$ indicates mass flux from ecosystem component X to Y. Fluxes are grouped by type as indicated.

guide the collection of observations which can be used for validating the model. Towards these ends, two complementary aspects are considered: (i) the sensitivity of the predicted ecological state variables to variations in the parameters, and (ii) the extent to which observations of the state variables allow us to determine the parameters. Omlin et al. (2001) further discusses aspects of parameter estimation in ecological prediction.

The ecosystem model is governed by the deterministic map given by (14). The central quantity used here to examine properties of the ecological model is the Jacobian matrix of partial derviatives,

$$J = \left.\frac{\partial f}{\partial \theta}\right|_{\theta=\hat{\theta}} \tag{15}$$

Table 3
Sensitivity of the ecosystem state variables in each of the boxes (columns) to variations in model parameters (rows)

	P1	P2	P3	Z1	Z2	Z3	N1	N2	N3	D1	D2	D3	B1	B2	B3
P_∞	8 (10)	6 (8)	7 (9)	1 (1)	1 (2)	1 (1)	1 (1)	2 (2)	2 (2)	0 (0)	1 (1)	1 (1)	1(3)	2(3)	1(3)
Z_∞	3 (3)	5 (7)	5 (6)	9 (9)	9 (8)	9 (9)	1 (1)	2 (2)	2 (2)	0 (0)	0 (0)	0 (0)	0(1)	0(2)	0(2)
N_∞	2 (2)	3 (3)	3 (3)	0 (0)	0 (0)	0 (0)	8 (8)	6 (6)	7 (7)	0 (0)	0 (0)	0 (0)	0(0)	1(1)	1(1)
D_∞	3 (2)	5 (4)	5 (4)	0 (0)	1 (1)	1 (1)	1 (2)	2 (2)	2 (2)	8 (8)	7 (5)	7 (6)	11(11)	10(9)	9(10)
γ_p	5 (5)	7 (11)	7 (9)	1 (1)	1 (2)	1 (2)	3 (3)	5 (5)	4 (4)	0 (0)	1 (1)	1 (1)	1(1)	1(5)	1(3)
Q_{10}	3 (2)	5 (4)	5 (3)	0 (0)	1 (1)	1 (0)	1 (1)	2 (2)	2 (2)	1 (1)	3 (2)	3 (2)	2(1)	4(2)	3(2)
K_∞	3 (2)	2 (1)	3 (1)	0 (1)	1 (1)	1 (1)	2 (2)	1 (1)	1 (1)	1 (2)	1 (1)	1 (1)	1(2)	1(2)	1(2)
K_{12}	0 (0)	3 (2)	0 (0)	0 (0)	1 (1)	0 (0)	0 (0)	2 (2)	0 (0)	0 (0)	1 (1)	0 (0)	0(0)	1(2)	0(0)
K_{13}	0 (0)	0 (0)	2 (1)	0 (0)	0 (0)	0 (1)	0 (0)	0 (0)	1 (1)	0 (0)	0 (0)	1 (1)	0(0)	0(0)	1(2)
λ_p	2 (2)	4 (3)	4 (3)	0 (0)	1 (0)	0 (0)	1 (0)	1 (1)	1 (1)	0 (0)	1 (0)	1 (0)	0(0)	1(1)	1(0)
I_z	5 (4)	8 (9)	7 (8)	2 (1)	3 (2)	3 (2)	2 (2)	3 (3)	3 (2)	0 (0)	0 (0)	0 (0)	0(1)	1(3)	1(2)
k_p	2 (2)	2 (4)	2 (4)	0 (0)	1 (1)	1 (1)	1 (1)	1 (1)	1 (1)	0 (0)	0 (0)	0 (0)	0(0)	0(1)	0(1)
λ_z	1 (1)	2 (3)	2 (2)	2 (2)	4 (4)	4 (3)	0 (0)	1 (1)	1 (1)	0 (0)	0 (0)	0 (0)	0(0)	0(1)	0(1)
ϵ_z	2 (1)	3 (3)	3 (2)	2 (1)	4 (3)	4 (3)	0 (0)	1 (1)	1 (0)	0 (0)	1 (0)	1 (0)	1(0)	1(1)	1(1)
β_z	1 (0)	1 (1)	1 (1)	0 (0)	0 (0)	0 (0)	0 (0)	0 (0)	0 (0)	0 (0)	1 (0)	1 (0)	0(0)	1(0)	1(0)
λ_d	0 (0)	0 (0)	0 (0)	0 (0)	0 (0)	0 (0)	0 (0)	0 (0)	0 (0)	1 (0)	1 (1)	1 (1)	12(3)	14(2)	12(2)
ϕ_d	3 (2)	5 (4)	5 (3)	0 (0)	1 (1)	1 (0)	1 (1)	2 (2)	2 (2)	1 (1)	3 (2)	3 (2)	2(1)	4(2)	3(2)
D_{in}	1 (1)	1 (1)	1 (1)	0 (0)	0 (0)	0 (0)	0 (0)	1 (1)	1 (1)	1 (1)	2 (2)	2 (2)	1(1)	3(3)	3(3)
$r(t)$	0 (0)	0 (1)	0 (1)	0 (0)	0 (0)	0 (0)	0 (0)	0 (0)	0 (0)	1 (2)	1 (3)	1 (3)	5(5)	7(5)	5(5)
N_{in}	1 (0)	2 (2)	1 (1)	0 (0)	0 (0)	0 (0)	0 (0)	1 (1)	0 (0)	0 (0)	0 (0)	0 (0)	0(0)	0(1)	0(0)
k_n	2 (2)	3 (5)	3 (4)	0 (0)	1 (1)	1 (1)	1 (1)	2 (2)	2 (2)	0 (0)	0 (0)	0 (0)	0(1)	1(2)	1(2)
α	0 (0)	0 (1)	0 (1)	0 (0)	0 (0)	0 (0)	0 (0)	0 (0)	0 (0)	0 (0)	0 (0)	0 (0)	3(8)	4(8)	3(8)
ϕ_b	0 (0)	0 (1)	0 (1)	0 (0)	0 (0)	0 (0)	0 (0)	0 (0)	0 (0)	0 (0)	0 (0)	0 (0)	1(2)	1(1)	1(1)
I_m	−(3)	−(7)	−(6)	−(0)	−(1)	−(1)	−(1)	−(1)	−(1)	−(2)	−(4)	−(4)	−(9)	−(6)	−(6)
ϵ_m	−(0)	−(0)	−(0)	−(0)	−(0)	−(0)	−(0)	−(0)	−(0)	−(0)	−(0)	−(0)	−(2)	−(2)	−(2)
β_m	−(0)	−(1)	−(1)	−(0)	−(0)	−(0)	−(0)	−(0)	−(1)	−(0)	−(0)	−(0)	−(1)	−(2)	−(2)

Results for the $M = 0$ and $M \neq 0$ cases are given, with $M \neq 0$ in brackets. For presentation purposes, values for S are scaled by a factor of 10, and rounded to the nearest integer.

which is evaluated for a specific parameter set $\theta = \hat{\theta}$. It takes the forms of an $q \times p$ matrix where the i, jth element is $\partial f_i/\partial\theta_j$, for $i = 1, \ldots, q$ and $j = 1, \ldots p$. It provides a linearization of the ecological dynamics about $\hat{\theta}$. Appendix B provides further details. Here, J was evaluated for both the $M = 0$ and $M \neq 0$ cases.

Sensitivity analysis identifies influential parameters in the nonlinear ecosystem model. The idea is to look at changes in the ecological state variables brought about by small perturbations in the parameters. The kth column of J, denoted J_k, measures the sensitivity of the ecosystem components X to variations in the kth parameter, θ_k. For the purposes of sensitivity analysis, a scaled Jacobian, denoted $\tilde{J}$ is used where $\tilde{J}_{ij} = (\theta_j/X_i)J_{ij}$. The measure of sensitivity is then

$$S_k^{(a,b)} = \langle |H_k^{(a,b)} \tilde{J}_k| \rangle. \tag{16}$$

Here, $|\cdot|$ represents the absolute value and $\langle\cdot\rangle$ provides for an averaging of the time series. The quantity $S_k^{(a,b)}$ measures the ratio of the percentage change in the model solution to a percentage change in a single parameter, following the usual definition (e.g., Jorgensen, 1994). It is computed for all 5 ecosystem components (superscript a) in all three boxes (superscript b) for each of the parameters contained in θ.

Results from the sensitivity analysis are shown in Table 3. For the $M = 0$ case, pelagic ecosystem components in all boxes are sensitive to their respective far-field concentrations. The far-field D_∞ also influences the level of the benthic detrital pool B. P in the inner boxes 2 and 3 are sensitive to γ_p as well as to I_z. The sinking rate λ_d, and to a lesser extent resuspension $r(t)$, are sensitive parameters in setting the level of B. Table 3 also shows results for the $M \neq 0$ case. Here, parameter sensivity for the pelagic components remains relatively unchanged. The exception is γ_p which is now important for P in the inner boxes, reflecting the increasing importance of internal production in the poorly flushed inner regions as grazing activity is increased. However,

Table 4
Estimated parameter precision reported as the ratio of the mean parameter value to its standard deviation

	ALL	P	Z	N	D	B
P_∞	2.99(1.69)	0.31 (0.71)	0.00 (0.00)	0.09 (0.16)	0.02 (0.08)	0.39 (0.07)
Z_∞	1.08(1.03)	0.00 (0.01)	0.27 (0.57)	0.01 (0.01)	0.00 (0.00)	0.04 (0.00)
N_∞	4.45(3.32)	0.03 (0.07)	0.00 (0.00)	1.50 (1.91)	0.01 (0.08)	0.41 (0.05)
D_∞	8.64(7.19)	0.00 (0.02)	0.00 (0.00)	0.04 (0.04)	1.64 (3.12)	1.69 (0.28)
γ_p	1.77(1.04)	0.06 (0.17)	0.01 (0.00)	0.10 (0.12)	0.01 (0.08)	0.30 (0.08)
K_∞	2.85(0.94)	0.07 (0.23)	0.03 (0.03)	0.21 (0.22)	0.22 (0.17)	0.89 (0.10)
K_{12}	2.73(0.85)	0.08 (0.19)	0.02 (0.03)	0.16 (0.20)	0.12 (0.11)	0.73 (0.07)
K_{13}	2.95(0.79)	0.09 (0.19)	0.02 (0.02)	0.17 (0.20)	0.14 (0.13)	0.79 (0.07)
λ_p	0.43(0.87)	0.00 (0.01)	0.00 (0.00)	0.01 (0.03)	0.01 (0.06)	0.07 (0.03)
I_z	0.69(0.61)	0.00 (0.01)	0.00 (0.00)	0.01 (0.01)	0.00 (0.00)	0.04 (0.00)
k_p	0.50(0.31)	0.01 (0.04)	0.00 (0.00)	0.04 (0.03)	0.00 (0.01)	0.07 (0.01)
λ_z	0.29(0.27)	0.01 (0.02)	0.03 (0.03)	0.01 (0.01)	0.00 (0.00)	0.04 (0.00)
ϵ_z	0.37(0.35)	0.00 (0.01)	0.00 (0.00)	0.01 (0.01)	0.00 (0.02)	0.14 (0.01)
β_z	0.39(0.35)	0.01 (0.03)	0.00 (0.00)	0.02 (0.03)	0.00 (0.01)	0.10 (0.01)
λ_d	0.67(2.36)	0.00 (0.01)	0.00 (0.00)	0.00 (0.02)	0.00 (0.29)	0.11 (0.23)
ϕ_d	3.47(1.12)	0.00 (0.02)	0.00 (0.00)	0.03 (0.04)	0.37 (0.43)	1.24 (0.15)
D_{in}	1.01(0.57)	0.00 (0.00)	0.00 (0.00)	0.02 (0.02)	0.05 (0.04)	0.28 (0.02)
$r(t)$	13.02(6.37)	0.00 (0.03)	0.00 (0.00)	0.04 (0.04)	1.90 (1.02)	8.86 (4.96)
N_{in}	1.28(0.45)	0.02 (0.08)	0.00 (0.00)	0.13 (0.18)	0.01 (0.05)	0.63 (0.05)
k_n	0.92(0.59)	0.02 (0.07)	0.00 (0.00)	0.12 (0.27)	0.01 (0.03)	0.20 (0.02)
α	1.37(0.24)	0.00 (0.02)	0.00 (0.00)	0.02 (0.02)	0.00 (0.03)	0.53 (0.01)
ϕ_b	0.26(0.05)	0.00 (0.01)	0.00 (0.00)	0.02 (0.01)	0.00 (0.01)	0.10 (0.00)
I_m	2.34(0.01)	0.00 (0.00)	0.00 (0.00)	0.01 (0.00)	0.01 (0.00)	0.60 (0.00)
ϵ_m	0.21(0.00)	0.00 (0.00)	0.00 (0.00)	0.00 (0.00)	0.00 (0.00)	0.06 (0.00)
β_m	0.26(0.00)	0.00 (0.00)	0.00 (0.00)	0.01 (0.00)	0.00 (0.00)	0.06 (0.00)

The column 'ALL' refers to observations available for all ecosystem state variables. The remaining columns assume that observations only on the variable indicated are available. Results are reported for both the $M = 0$ and $M \neq 0$ cases, with $M \neq 0$ in brackets.

it is the benthos B which shows the greatest changes. There is increased sensitivity in B to burial α, but much less sensitivity to sinking λ_d. The importance of biodeposition is made evident by the fact I_m strongly influences P in the inner boxes, and is also important in determining B.

To determine how the ecosystem state variables are related to the parameters the asymptotic error covariance matrix, Σ, for the parameters was determined. This used the Jacobian matrix in (15) together with some basic principles in nonlinear regression, as outlined in Appendix B. Examining Σ shows the extent to which information on the ecosystem state variables allows us to determine model parameters, and hence predict the ecosystem state. The diagonal elements of Σ provide an estimate for the variance of the model parameters θ. The off-diagonal elements provides information on how they are related, or covary. It is important to note that we do not need actual observations for this exercise; only information on which variables are measured and their error statistics is required (see Appendix B). Here, the covariance matrix Σ was computed assuming a complete set of observations on the ecosystem state, X, as well as for limited sets of observations, i.e. $X^{(a,b)}$. For simplicity, a unit variance for the observation errors was assumed, which is reasonable starting point for variables having the same order of magnitude. However, in reality, observation errors will be unequal and depend on sampling variability and measurement precision.

Table 4 shows information on parameter uncertainty. These are reported as the ratio of the parameter values to their estimated standard deviation, and can be interpreted as a measure of the relative precision of the parameters. First, consider the situation where a complete set of observations of X is available (the 'ALL' column in Table 4). For both the $M = 0$ and $M \neq 0$ cases, it is seen that the far-field pelagic components are well determined, as are the parameters for resuspension and water column remineralization. In contrast, parameters associated with Z tend to be

Table 5
Estimated correlation matrix for the parameters for both the $M = 0$ case (above main diagonal) and the $M \neq 0$ case (below main diagonal)

	P_∞	Z_∞	N_∞	D_∞	γ_p	K_∞	K_{12}	K_{13}	λ_p	I_z	k_p	λ_z	ϵ_z	β_z	λ_d	ϕ_d	D_{in}	$r(t)$	N_{in}	k_n	α	ϕ_b	I_m	ϵ_m	β_m
P_∞	•	2	0	0	−4	−1	−4	−2	0	2	2	1	−1	1	0	0	6	0	−2	−4	1	−1	6	7	−2
Z_∞	2	•	−1	0	−1	−1	0	0	0	0	1	7	1	−1	0	0	1	0	0	0	0	0	1	1	0
N_∞	−3	0	•	0	−2	4	0	0	−1	4	4	−5	−7	6	−1	1	−3	0	1	−3	2	−2	−4	1	−7
D_∞	−2	0	−1	•	0	0	0	0	0	0	0	0	0	0	−2	0	−3	0	0	0	0	0	0	0	0
γ_p	−1	−2	−1	−1	•	2	4	4	6	−4	−5	1	2	−2	2	3	0	0	2	7	0	0	0	−4	5
K_∞	−3	−1	2	−3	−1	•	5	4	4	1	−1	0	−1	−1	0	8	0	1	3	−2	1	−1	−4	−2	−2
K_{12}	−2	−1	−1	5	−1	1	•	7	4	−1	−3	1	2	−3	1	6	−2	0	7	1	0	0	−5	−4	0
K_{13}	−2	0	−1	5	−1	1	9	•	4	−1	−3	2	2	−3	0	6	0	1	2	0	0	1	−3	−4	1
λ_p	5	0	−2	−3	5	−1	−1	−1	•	−2	−4	1	1	0	4	4	0	0	2	2	0	0	−2	−3	2
I_z	3	2	3	−1	−3	0	0	−1	−3	•	9	−2	−6	5	0	0	0	0	−1	−7	2	−2	0	1	−2
k_p	1	2	4	0	−5	1	0	0	−4	9	•	−3	−5	5	0	−2	0	0	−1	−6	2	−2	0	2	−3
λ_z	3	8	−4	0	−1	−1	1	1	1	−1	−2	•	7	−6	0	1	1	0	0	1	−2	2	1	−2	4
ϵ_z	0	1	−6	1	0	0	2	2	3	−6	−6	6	•	−8	0	1	1	0	0	3	−3	3	0	−4	5
β_z	2	−1	5	−1	1	−1	−1	−1	3	3	4	−5	−7	•	1	−4	−2	0	−1	−3	2	−3	0	3	−4
λ_d	8	1	−3	−4	1	−2	−2	−2	6	2	−1	2	1	1	•	−1	−2	−2	1	0	0	0	−3	−2	2
ϕ_d	−3	−1	−2	0	1	4	2	2	−3	−2	−2	0	2	−5	−2	•	3	1	3	−1	2	−1	−1	−1	−1
D_{in}	2	−1	−2	−3	4	−1	−4	−4	1	−2	−4	−1	0	−2	2	5	•	0	−3	−1	2	−2	8	7	1
$r(t)$	1	0	−1	−1	0	−2	−1	−1	0	−1	−2	1	2	−2	3	−1	1	•	0	0	0	0	0	0	0
N_{in}	1	−2	−1	4	−3	−1	6	7	0	1	1	−1	1	−1	0	0	−4	0	•	1	1	−1	−5	−2	−3
k_n	−5	−1	−1	1	7	−1	−1	0	0	−4	−4	−1	1	0	−3	1	2	0	−3	•	−1	1	0	−3	4
α	−2	0	−1	1	−2	0	1	1	−3	3	3	−2	−4	2	−2	1	0	−2	1	−2	•	−9	1	1	1
ϕ_b	1	−1	1	−1	2	1	−1	−1	3	−3	−3	2	4	−2	2	−1	1	3	−1	1	−9	•	−1	−1	−1
I_m	−4	−2	−1	1	3	1	0	1	−3	−4	−4	−2	0	−3	−4	6	7	0	−2	4	1	0	•	7	2
ϵ_m	2	−1	3	−1	3	−1	−2	−2	2	−1	−2	−2	−1	1	2	2	6	2	−1	1	−6	6	4	•	−5
β_m	1	1	−6	0	0	0	1	1	0	0	0	2	2	−2	1	1	0	−1	0	−1	7	−7	0	−8	•

For presentation purposes, correlations have been multiplied by a factor of 10, and the main diagonal is represented by a "•".

poorly determined. Comparing the $M = 0$ and $M \neq 0$ cases indicates that the precision of nearly all parameters increases with greater bivalve biomass. This is particularly evident for the exchange coefficients, the mussel parameters, and all parameters associated with benthic–pelagic coupling. The exceptions are λ_d and λ_p. The remaining columns in Table 4 report precision estimates where observations on only one ecosystem component is available. As expected, the precision is reduced with the tendency that only parameters directly linked to the observables are well determined. Observations of pelagic variables are more important for the $M = 0$ case, while observations of the benthic detrital pool are relatively more important for the $M \neq 0$ case.

The estimated correlation matrix for the parameters is shown in Table 5. Correlation measures the linear dependence amongst the parameters. A value close to zero indicates parameters are nearly independent. Absolute values near one indicates parameters may not be independent, i.e. varying these parameters can lead to a similar model predictions for the time evolution of the state variables. Correlations were computed for cases with $M = 0$ (above the main diagonal) and $M \neq 0$ (below the main diagonal), assuming a full observation set. For both cases, the majority of parameters have relatively low correlations (< 0.5); high correlations are evident only amongst the Z parameters, between the D source/sink terms (I_m, D_{in}), and between the B loss terms (α, ϕ_b). For the $M \neq 0$ case, high correlations are evident amongst the M parameters, the source/sink and loss terms for Z (Z_∞, λ_z) and P (P_∞, λ_p), and the interior exchange coefficients (K_{12}, K_{13}). Examination of the eigenvalues and eigenvectors of the covariance and correlation matrices did not prove informative as a means of identifying important parameter dependencies.

5. Summary and conclusions

This study has presented a bio-physical ecosystem model for assessing environmental effects of intensive bivalve culture in shallow coastal bays. It is motivated by the potential of dense aggregates of bivalves to deplete suspended particulates and increase biodeposition (Cloern, 1982; Dame and Prins, 1998; Noren et al., 1999). This can alter nutrient cycling in coastal ecosystems (Hily, 1991; Alpine and Cloern, 1992). Ecosystem effects have been widely documented for cases where bivalve populations have exploded as invasive species (Nichols, 1985; Nichols et al., 1990), or have been decimated as a result of disease (Ulanowicz and Tuttle, 1992). Bivalves have been termed "ecosystem engineers" as a result of this ability to alter environmental conditions in their favour (Jones et al., 1994; Seed, 2000).

Quantitative approaches are useful for examining aquaculture ecosystems and environmental management (Kishi et al., 1994). Brando et al. (2004) presents a mass balance model of trophic flows for management of a lagoon system as an extensive aquaculture operation. Congleton et al. (1999) considers a spatial modelling framework to take account habitat variability in siting bivalve aquaculture. A population dynamics model of clam culture is developed by Solidoro et al. (2003) and coupled to one of individual bio-energetics; this was applied to the identification of rearing strategies to balance ecological and economic considerations. Ecosystem models of bivalve aquaculture ecosystems have been focused mainly on predicting bivalve growth and carrying capacity. One approach is to couple bivalve bioenergetic models with models of the supporting marine ecosystem (Raillard and Ménesguen, 1994; Dowd, 1997). Increasingly the trend is to integrate complex ecosystem and bioenergetic models with physical models of hydrodynamic processes (Solidoro et al., 2000; Duarte et al., 2003). In our study, we emphasize environmental effects of bivalve culture. Towards this end, we identify a general mathematical modelling framework for quantifying ecosystem effects of bivalve aquaculture from a nutrient cycling perspective.

The bio-physical model used in this study describes the dynamics of interacting populations in a semi-enclosed embayment. The focus is on variability on subtidal time scales, with a particular emphasis on seasonal effects. Spatial aspects are incorporated using a box model framework which allows for redistribution of ecosystem components by water motion and mixing. The pelagic compartment is comprised of phytoplankton, zooplankton, nutrients and detritus in keeping with current representations used in modelling pelagic biogeochemistry (Fasham, 1993). The model was targeted at shallow coastal systems by coupling the pelagic components to a simple, but dynamically active, benthos. Novel aspects for the benthic compartment includes episodic resuspension of benthic detritus based on a

stochastic (Poisson) process consistent with wind forcing; the model ecosystem appears to be resilient to these short time scale perturbations, in the sense defined by Stone et al. (1996). In addition, remineralization of benthic detritus was represented using a convolution integral which mimics the effects of finite reaction times and sediment pore water diffusion as represented in complex diagenetic models such as those in Soetaert et al. (2000). Considerable dynamical simplification was also achieved by superimposing a fixed population of grazing bivalves which interacts with the ecosystem as a forcing function.

A specific case study was undertaken for Tracadie Bay, a shallow semi-enclosed tidal embayment off the east coast of Canada. The purpose was to illustrate application of the general model to a specific situation, as well as to generate and test some hypotheses on potential ecosystem effects resulting from intensive bivalve culture. Recently, an extensive bio-physical field study of Tracadie Bay was initiated, and this work provides an initial application to help focus the field program and interpret results. At this stage we make use of preliminary observations, information from regional databases and reports, and literature values to specify model inputs, as well as to calibrate the model output.

Effects of intensive bivalve culture were investigated by applying the aquaculture ecosystem model to cases both with and without a population of grazing bivalves. Zooplankton play only a minor role in nutrient cycling and, from this perspective, could be justifiably neglected (but are important if production at higher trophic level is of interest). Major ecosystem effects of bivalve populations are concentrated in the benthos where bivalve biodeposition leads to an accumulation of organic matter. Biological production is in fact diverted from the pelagic to the benthic food web. In the biologically active summer period, the dominant nutrient cycle is the following. Seston (phytoplankton and detritus) is depleted from the water column by grazing. Bivalves produce feces and pseudofeces from this ingested matter and which are rapidly biodeposited to the seabed. Benthic accumulation of organic detritus on the seabed enhances water column nutrients due to benthic remineralization. This drives increased phytoplankton production in this normally nutrient limited system. However, phytoplankton are simultaneously grazed down by bivalves so that their standing stock actually decreases. Coastal eutrophication thus appears to be partially mitigated by bivalve mediated sinks for excess nutrients, mainly the storage of biodeposited organic matter in the sediments and its burial (note that only a relatively small amount of nutrients are removed directly through harvesting). However, the major nutrient sink is through export to the offshore, consistent with the findings of Le Pape et al. (1999). The phytoplankton to detritus ratio may be thought of as a measure of food quality and is an important determinant of bivalve growth (Penney et al., 2001). Simulations suggest that bivalve populations increase this ratio and therefore alter the environmental conditions in their favor, consistent with their hypothesized role as ecosystem engineers. As the fall period progresses, internal biological dynamics in the bay are weak, the system moves from net autotrophic to heterotrophic, and bivalves increasingly rely on offshore production for their maintenance food ration.

In a semi-enclosed coastal embayment, ecological dynamics are determined both by local processes within the bay, as well as by the dynamics of the larger scale oceanic ecosystem. These local and remote forcings are linked through water motion, which redistributes and exchanges freely floating ecosystem components. The importance of this physical oceanographic aspect in structuring the ecological system led us to propose a unique means of determining the exchange coefficients based on an inversion of observed temperature records. This data-driven estimation of the mixing coefficients contrasts with other methods based on tidal prism calculations (Dowd, 1997) or analysis of numerical circulation model output (Chapelle et al., 2000; Thompson et al., 2002). The limited-area model used in this study clearly shows how far-field conditions influence the internal biological dynamics. Mixing processes may also lend stability to the ecosystem dynamics through the gradient-flux relation which governs exchange, similar to the way in which a pelagic ecosystem model can be stabilized by the addition of diffusive physics (Edwards et al., 2000). Water motion and mixing also means that the inner portions of the bay are decoupled from the far-field, and internal ecosystem processes play a relatively more important role there (Dowd, 2003).

The aquaculture ecosystem model presented in this paper is intended to be applied to similar situations

with minor modification to its basic structure. Towards this end, an brief analysis of some model properties was undertaken. Since the model provides a deterministic map from the parameters to the ecosystem state variables, we examined aspects of parameter estimation using quantities derived from the Jacobian matrix of partial derivatives. Overall, the parameter sensitivity was found to be fairly uniform. More sensitive parameters were associated with the major pathways of mass flow in the system, i.e. the mussel energy balance parameters and the parameters governing benthic–pelagic coupling. More sophisticated sensitivity analysis for ecological models considers interactions, or dependencies, amonst the parameters (Omlin et al., 2001; Beres and Hawkins, 2001; Barlund and Tattari, 2001). To address such parameter identification and uncertainty issues, we computed the asymptotic covariance matrix for the parameters, assuming availability of observations on some or all of the ecological state variables. The covariance matrix is the inverse of the Hessian matrix, which was used by Marsili-Libelli et al. (2003) to determine confidence regions for ecological parameters. Not surprisingly, it was found that parameter variances, or precision, estimates were often dependent on having direct observations of the associated state variable. The majority of parameters turned out to be quasi-independent for this estimation problem which is encouraging for future applications. Only minor differences in the covariance structure were evident for the two bivalve population levels considered.

Quantitative descriptions of aquaculture ecosystems are important tools to further the scientific understanding and the management of these manipulated ecosystems. Parsimonious models of such inherently complex ecological systems, such as the approach offered in this study, offer simplicity by including only dominant processes and by using reliable, robust parameterizations and approximations. Although some realism is sacrified for generality, there are important advantages over their highly complex and case-specific counterparts: simple models are more easily validated, their dynamical properties can be better understood and analysed, and hypotheses can be systematically tested. Such models thus both complement, and provide the basis for, the more complex systems-based models in ecology (see Wu and Marceau, 2002). However, another reason exists for using simple, but non-trival, biological models: they provide a practical basis to investigate emerging areas in predictive ecosystem modelling which are presently characterised by formidable compuational requirements. In ecological modelling, these include stochastic simulation (Marion et al., 2000) and inverse problems (Vallino, 2000; Dowd and Meyer, 2003). In marine ecology specifically, a major thrust is the coupling of biological dynamics to high dimension, fluid dynamical models of ocean circulation (Hofmann and Lascara, 1998). It is hoped that the bio-physical ecosystem model proposed in this study proves useful, both for its present practical application, as well as for future developments towards the goal of predictive marine ecosystem modelling.

Acknowledgements

The author would like to thank Dr. Alain Vezina of the Bedford Institute of Oceanography, Dr. Jon Grant of Dalhousie University and Dr. Cedric Bacher of IFREMER for discussions on the modelling of coastal ecosystems. Drs. Peter Cranford, Peter Strain, Paul Kepkay and Fred Page of Fisheries & Oceans Canada are also acknowledged for their contributions and support in the ongoing field activities in Tracadie Bay. This work was supported by Fisheries & Oceans Canada through their Environmental Sciences Strategic Research Fund. The author was supported by an NSERC Discovery Grant.

Appendix A. Determining the exchange coefficients

To implement the ecosystem box model (11)–(13) requires numerical values for the three exchange coefficients: K_{∞}, K_{12}, K_{13}. These were determined using observed temperature time series for each of the boxes, designated $\mathrm{Temp}_1(t)$, $\mathrm{Temp}_2(t)$ and $\mathrm{Temp}_3(t)$, respectively. Fig. 9a shows the observed low frequency temperature variations recorded in summer 1999 in Tracadie Bay. These have been zero-phase, low pass filtered with 100 h cutoff to eliminate tidal variations. This procedure is consistent with considering only subtidal variability in the box model. The major feature in the temperature regime of the bay is a spatial gradient of a few degrees Celsius: the temperature in offshore waters (Temp_{∞}) is lower than the central bay

(Temp_1), which is in turn cooler than the inner regions (Temp_2 and Temp_3).

The time evolution of temperature can be modelled by transforming (11)–(13) into a heat equation as follows. Let $X_i = \text{Temp}_i$ and $h\{\cdot\} = 0$. The term ν is interpreted as a heating rate common to all boxes. A typical summer value for the net heat flux for the region is $150\,\text{W m}^{-2}$ according to the NCEP/NCAR 40 year global heat flux analysis for this area in the months July and August, as reported in Kalnay et al. (1996). The heating rate is $\nu = \Phi/(H\rho C_p)$, where $\Phi = 150\,\text{W m}^{-2}$ is the input heat flux, $C_p = 4000\,\text{J kg}^{-1}\,^\circ\text{C}^{-1}$ is the specific heat of seawater, and $\rho = 1025\,\text{kg m}^{-3}$ is the density of seawater. Using a water column of depth $\eta = 5\,\text{m}$ yields a heating rate of $0.75\,^\circ\text{C d}^{-1}$. An inverse method was used to determine the exchange coefficients. Specifically, the scalar quantity

$$\Psi = \sum_i \left\{ \int_t (\text{Temp}_i(t) - \widehat{\text{Temp}}_i(t))^2 \, dt \right\} \tag{17}$$

was minimized with respect to K_∞, K_{12}, K_{13}. This minimization is subject to the predicted $\widehat{\text{Temp}}_i$ satisfying the heat equation. In other words, the exchange coefficients are chosen such that they provide predicted temperatures which best fit, in a least squares sense, the observations. Carrying out the above procedure resulted in the following estimates for the exchange coefficients: $\hat{K}_\infty = 1.3\,\text{d}^{-1}$, $\hat{K}_{12} = 0.4\ \text{d}^{-1}$, an $\hat{K}_{13} = 0.5\,\text{d}^{-1}$. These values were used in the box model. The associated predicted temperatures are given in Fig. 9b.

Appendix B. Model analysis using nonlinear regression

Consider the nonlinear regression equation

$$y = Hf\{\theta\} + \varepsilon \tag{18}$$

where y represents a $k \times 1$ vector of observations on the ecosystem state variables and θ is the $p \times 1$ parameter vector. The $q \times 1$ vector function $f\{\cdot\}$ operates on θ and corresponds to the discretized ecosystem dynamics as in (14). The $k \times q$ matrix H picks out model counterparts to the observations (note that the case where $H = I$ implies measurements of all ecosystem components in all boxes at all model time steps). The $k \times 1$ error vector ε is assumed, for simplicity, to be independent, zero-mean and normally distributed with common variance σ^2. Ordinary least squares nonlinear regression is concerned with choosing an estimate for θ so as to minimize the error sum of squares $S(\theta) = \|y - Hf\{\theta\}\|^2$. The interested reader is referred to Chapter 24 of Draper and Smith (1998) for a more detailed introduction to this problem.

Here, we are concerned with an examination of the properties of this estimation problem independent of any particular set of observations. That is, we use only knowledge of the observing array (H) and the error statistics ($\varepsilon \sim N(0, \sigma^2 I)$). Suppose then we have an estimate $\hat{\theta}$ obtained by either minimizing $S(\theta)$, or simply as a prescribed baseline parameter set. A linearization (truncated Taylor series) of $f\{\theta\}$ about $\hat{\theta}$ yields

$$f(\theta) = f\{\hat{\theta}\} + \left.\frac{\partial f}{\partial \theta}\right|_{\theta=\hat{\theta}} (\theta - \hat{\theta}). \tag{19}$$

The Jacobian matrix of partial derivatives is given by the $q \times p$ matrix $J = \partial f/\partial\theta$. Its i, jth element is defined as

$$\frac{\partial f_i}{\partial \theta_j} = \lim_{\Delta\theta_j \to 0} \frac{1}{\Delta\theta_j} (f_i\{\theta + \Delta\theta_{(j)}\} - f_i\{\theta\}) \tag{20}$$

where $\Delta\theta_{(j)}$ is a $p \times 1$ vector with all zero elements excepting the jth element, $\Delta\theta_j$. Using the formula (20), J is readily approximated using finite differences (e.g. Gill et al., 1986, Section 8.6).

Define the increments $\delta y = y - f\{\hat{\theta}\}$ and $\delta\theta = \theta - \hat{\theta}$. The linear regression $\delta y = HJ\delta\theta + \delta\varepsilon$, which is localized about $\hat{\theta}$, yields

$$\widehat{\delta\theta} = \Sigma J' H' \delta y \tag{21}$$

where

$$\Sigma = (J' H' H J)^{-1}.$$

assuming the quantity in brackets is non-singular. The quantity $\sigma^2\Sigma$ represents the covariance matrix for $\widehat{\delta\theta}$. It also provides an approximate covariance matrix for $\hat{\theta}$ asymptotically valid in the vicinity of $\hat{\theta}$. The $p \times 1$ vector of parameter variances is then

$$\text{var}(\hat{\theta}) = \sigma^2 \,\text{diag}(\Sigma). \tag{22}$$

A linearized correlation matrix Γ for the θ can also be defined. This $p \times p$ matrix has elements

$$\Gamma_{ij} = \frac{\Sigma_{ij}}{(\Sigma_{ii} \times \Sigma_{jj})^{1/2}} \quad (23)$$

for $i, j = 1, \ldots, p$. The eigenvalues and eigenvectors of Σ, or Γ, may prove useful in identifying parameters sets which are poorly determined by available observations.

References

Alpine, A.E., Cloern, J.E., 1992. Trophic interactions and direct physical effects control phytoplankton biomass and production in an estuary. Limnol. Oceanogr. 37, 946–955.

Barlund, I., Tattari, S., 2001. Ranking of parameters on the basis of their contribution to model uncertainty. Ecol. Modell. 142, 11–23.

Beres, D.L., Hawkins, D.M., 2001. Plackett-Burman technique for sensivity analysis of many parametered models. Ecol. Modell. 141, 171–183.

Berner, R.A., 1964. An idealized model of dissolved sulphate distribution in recent sediments. Geochim. Cosmochim. Acta 28, 1497–1503.

Boudreau, B.P., 1997. Diagenetic Models and Their Implementation. Modeling Transport and Reactions in Aquatic Sediments. Springer, Berlin 414.

Boyce, W.E., DiPrima, R.C., 1986. Elementary Differential Equations and Boundary Value Problems. John Wiley & Sons, New York 654.

Brando, V.E., Ceccarelli, R., Libralatos, S., Ravagnan, G., 2004. Assessment of environment management effects in a shallow water basin using mass balance models. Ecol. Modell. 172, 213–232.

Caperon, J., 1967. Population growth in micro-organisms limited by food supply. Ecology 48, 715–722.

Carver, C.E.A., Mallet, A.L., 1990. Estimating the carrying capacity of a coastal inlet for mussel culture. Aquaculture 88, 39–53.

Chapelle, A., Ménesguen, A., Deslous-Paoli, J.-M., Souchu, P., Mazouni, N., Vaquer, A., Millet, B., 2000. Modelling nitrogen, primary production and oxygen in a Mediterranean lagoon. Impact of oysters farming and inputs from the watershed. Ecol. Modell. 127, 161–181.

Cloern, J.E., 1982. Does the benthos control phytoplankton biomass in southern San Francisco Bay? Mar. Ecol. Prog. Ser. 9, 191–202.

Congleton, W.R., Pearce, B.R., Parker, M.R., Beal, B.F., 1999. Mariculture siting: a GIS description of intertidal areas. Ecol. Modell. 116, 63–75.

Cranford, P., Dowd, M., Grant, J., Hargrave, B., McGladdery, S., 2002. Ecosystem level effects of marine bivalve aquaculture. In: Volume I: A scientific review of the potential environmental effects of aquaculture in aquatic acosystems. Canadian Technical Report of Fisheries and Aquatic Sciences, vol. 2450, pp. 51–84.

Crawford, C.M., MacLeod, C.K.A., Mitchell, I.A., 2003. Effects of shellfish farming on the benthic environment. Aquaculture 224, 117–140.

Dame, R.F., Dankers, N., Prins, T., Jongsma, H., Smaal, A., 1991. The influence of mussel beds on nutrients in the West Wadden Sea and Eastern Scheldt estuaries. Estuaries 14, 130–138.

Dame, R.F., Prins, T.C., 1998. Bivalve carrying capacity in coastal ecosystems. Aquat. Ecol. 31, 409–421.

Dowd, M., 1997. On predicting the growth of cultured bivalves. Ecol. Modell. 104, 113–131.

Dowd, M., 2003. Seston dynamics in a tidal embayment with shellfish aquaculture: a model study using tracer equations. Estuarine Coast. Shelf Sci. 57, 523–537.

Dowd, M., Meyer, R., 2003. A Bayesian approach to the ecosystem inverse problem. Ecol. Modell. 168, 39–55.

Dowd, M., Page, F., Losier, R., 2002. Time series analysis of temperature, salinity, chlorophyll and oxygen data from Tracadie Bay, PEI. Canadian Technical Report of Fisheries and Aquatic Sciences, vol. 2441, pp. 86.

Dowd, M., Page, F., Losier, R., McCurdy, P., Budgen, G., 2001. Physical oceanography of Tracadie Bay, PEI: Analysis of sea level, current, wind and drifter data. Canadian Technical Report of Fisheries and Aquatic Sciences, vol. 2347, pp. 80.

Draper, N.R., Smith, H.S., 1998. Applied Regression Analysis. Wiley, New York 706.

Duarte, P., Meneses, R., Hawkins, A.J.S., Zhu, M., Fang, J., Grant, J., 2003. Mathematical modelling to assess the carrying capacity for multi-species culture within coastal waters. Ecol. Modell. 168, 109–143.

Dugdale, R.C., 1967. Nutrient limitation in the sea: dynamics, identification and significance. Limnol. Oceanogr. 12, 685–695.

Edelvang, K., Lund-Hansen, L.C., Christiansen, C., Peterson, O.S., Uhrenholdt, T., Laima, M., Berastegui, D.A., 2002. Modelling suspended matter transport from the Oder River. J. Coastal Res. 18, 62–74.

Edwards, A.M., 2001. Adding detritus to a nutrient-phytoplankton-zooplankton model: a dynamical systems approach. J. Plankton Res. 23, 389–413.

Edwards, C.A., Powell, T.A., Batchelder, H.P., 2000. The stability of an NPZ model subject to realistic levels of vertical mixing. J. Mar. Res. 58, 37–60.

Epply, R.W., 1972. Temperature and phytoplankton growth in the sea. Fish. Bull. 70, 1063–1085.

Evans, G.T., Parslow, J.S., 1985. A model of annual plankton cycles. Biol. Oceanogr. 3, 327–347.

Fasham, M.J.R., 1993. Modelling the marine biota. In: Heimann, M. (Ed.), The Global Carbon Cycle. Spinger-Verlag, Berlin 457–504.

Fasham, M.J.R., Ducklow, H.W., McKelvie, S.M., 1990. A nitrogen based model of plankton dynamics in the oceanic mixed layer. J. Mar. Res. 48, 591–639.

Fischer, H.B., List, E.J., Koh, R.C.Y., Imberger, J., Brooks, N.H., 1979. Mixing in Inland and Coastal Waters. Academic Press, New York 483.

Franks, P.J.S., Wroblewski, J.S., Flierl, G.R., 1986. Behaviour of a simple plankton model with food-level acclimation by herbivores. Mar. Biol. 91, 121–129.

Fréchette, M., Butman, C.A., Geyer, W.R., 1989. The importance of boundary layer flow processes in supplying phytoplankton to the benthic suspension feeder *Mytilus edulis* L. Limnol. Oceanogr. 34, 19–36.

Frost, B.W., 1975. A threshold feeding behaviour in Calanus pacificus. Limnol. Oceanogr. 20, 259–262.

Gardiner, C.W., 1997. Handbook of Stochastic Methods. Springer, Berlin 442.

Gill, P.E., Murray, W.E., Wright, M.H., 1986. Practical Optimization. Academic Press, London 401.

Grant, J., Hatcher, A., Scott, D.B., Pocklington, P., Schafer, C.T., Honig, C., 1995. A multidisciplinary approach to evaluating benthic impacts of shellfish aquaculture. Estuaries 18, 124–144.

Gregory, D., Petrie, B., Jordan, F., Langille, P., 1993. Oceanographic, geographic, and hydrological parameters of Scotia-Fundy and southern Gulf of St. Lawrence inlets. Canadian Technical Report of Hydrography and Ocean Sciences, vol. 143, pp. 248.

Griffiths, C.L., Griffiths, R.J., 1987. Bivalvia. In: Pandian, T.J., Vernberg, F.J. (Eds.), Animal Energetics. Bivalvia through Reptilia, Vol. 2. Academic Press, New York, pp. 2–87.

Hargrave, B.T., 1985. Particle sedimentation in the ocean. Ecol. Modell. 30, 229–246.

Hassell, M.P., 1978. The Dynamics of Arthropod Predator–Prey Systems. Princeton University Press, Princeton, pp. 237.

Hatcher, A., Grant, J., Schofield, B., 1994. Effects of suspended mussel culture (Mytilus spp.) on sedimentation, benthic respiration and sediment nutrient dynamics in a coastal bay. Mar. Ecol. Prog. Ser. 115, 219–235.

Heip, C.H.R., Goosen, N.K., Herman, P.M.J., Kromkamp, J., Middleburg, J.J., Soetaert, K., 1995. Production and consumption of biological particles in temperate tidal estuaries. Oceanogr. Mar. Biol.: Annu. Rev. 33, 1–149.

Hily, C., 1991. Is the activity of benthic suspension feeders a factor controlling water quality in the Bay of Brest? Mar. Ecol. Prog. Ser. 69, 179–188.

Hofmann, E.E., Lascara, C.M., 1998. Overview of interdisciplinary modeling for marine ecosystems. In: Brink, K.H., Robinson, A.R. (Eds.), The Sea: Ideas and Observations on Progress in the Study of the Seas. Volume 10: The Global Coastal Ocean: Processes and Methods. Wiley, New York.

Holling, C.S., 1959. The components of predation as revealed by a study of small mammal predation of the European pine sawfly. Can. Entomol. 91, 293–320.

Incze, L.S., Lutz, R.A., True, E., 1981. Modeling carrying capacities for bivalve molluscs in open suspended-culture systems. J. World Maricult. Soc. 12, 143–155.

Jones, C.G., Lawton, J.H., Shachak, M., 1994. Organisms as ecosystem engineers. Oikos 69, 373–386.

Jones, R., Henderson, E.W., 1986. The dynamics of nutrient regeneration and simulation studies of the nutrient cycle. Journal du Conseil 43, 216–236.

Jorgensen, S.E., 1994. Fundamentals of Ecological Modelling. Elsevier, Amsterdam 687.

Kalnay, E., Kanamitsu, M., Kistler, R., Collins, W., Deaven, D., Gandin, L., Iredell, M., Saha, S., White, G., Woollen, J., Zhu, Y., Chelliah, M., Ebisuzaki, W., Higgins, W., Janowiak, J., Mo, K.C., Ropelewski, C., Wang, J., Leetmaa, A., Reynolds, R., Jenne, R., Joseph, D., 1996. The NCEP/NCAR 40 year reanalysis project. Bull. Am. Meteorol. Soc. 77, 431–437.

Kaspar, H.F., Gillespie, P.A., Boyer, I.C., MacKenzie, A.L., 1985. Effects of mussel aquaculture on the nitrogen cycle and benthic communities in Kenepuru Sound, Marlborough Sound, New Zealand. Mar. Biol. 85, 127–136.

Kemp, W.M., Brooks, M.T., Hood, R.R., 2001. Nutrient enrichment, habitat variability and trophic transfer efficiency in simple models of pelagic ecosystems. Mar. Ecol. Prog. Ser. 223, 73–87.

Kishi, M.J., Uchiyama, M., Iwata, Y., 1994. Numerical simulation model for quantitative management of aquaculture. Ecol. Modell. 72, 21–40.

Kremer, J., Nixon, S.W., 1978. A Coastal Marine Ecosystem: Simulation and Analysis. Springer-Verlag, New York, pp. 217.

Le Pape, O., Jean, F., Ménesguen, A., 1999. Pelagic and benthic trophic chain coupling in a semi-enclosed coastal system, the Bay of Brest (France): a modelling approach. Mar. Ecol. Prog. Ser. 189, 135–147.

Marion, G., Renshaw, E., Gibson, G., 2000. Stochastic modelling of environmental variation for biological populations. Theor. Popul. Biol. 57, 197–217.

Marsili-Libelli, S., Guerrizio, S., Checchi, N., 2003. Confidence regions of estimated parameters for ecological systems. Ecol. Modell. 165, 127–146.

Middleburg, J.J., Soetart, K., Herman, P.M.J., 1997. Empirical relationships for use in global diagenetic models. Deep Sea Res. 44, 327–344.

New, M.B., 1999. Global aquaculture: current trends and challenges for the 21st century. World Aquacult. 30, 8–13.

Nichols, F.H., 1985. Increased benthic grazing: an alternative explanation for low phytoplankton biomass in northern San Francisco Bay during the 1976–1977 drought. Estuarine Coastal Shelf Sci. 21, 379–388.

Nichols, F.H., Thompson, J.K., Schemel, L.E., 1990. Remarkable invasion of San Francisco Bay (California, USA) by the Asian clam Potamocorbula amurensis. II. Displacement of a former community. Mar. Ecol. Prog. Ser. 66, 95–101.

Nisbet, R.M., Diehl, S., Wilson, W.G., Cooper, S.D., Donaldson, D.D., Kratz, K., 1997. Primary productivity gradients and short-term population dynamics in open systems. Ecol. Monogr. 67 (4), 535–553.

Noren, F., Haamer, J., Lindahl, O., 1999. Changes in the plankton community passing a Mytilus edulis bed. Mar. Ecol. Prog. Ser. 19, 187–194.

Omlin, M., Brun, R., Reichert, P., 2001. Biogeochemical model of Lake Zurich: sensitivity, identifiability and uncertainty analysis. Ecol. Modell. 141, 105–123.

Page, F., Greenberg, D., Bugden, G., Losier, R., Shore, J., Horne, E., Robinson, S., Chang, B., Sephton, T., 1999. Oceanographic component of the Canadian Department of Fisheries and Oceans science strategic research program on Coastal Oceanography for Sustainable Aquaculture Development (COSAD). Bull. Aquacult. Assoc. Can. 99–2, 14–16.

Parsons, T.R., Takahashi, M., Hargrave, B., 1977. Biological Oceanographic Process. Permagon, Oxford 220.

Pastres, R., Solidoro, C., Cossarini, G., Melaku Canu, D., Dejak, C., 2001. Managing the rearing of Tapes philippinarum in the

lagoon of Venice: a decision support system. Ecol. Modell. 138, 231–245.

Penney, R.W., McKenzie, C.H., Mills, T.J., 2001. Assessment of the particulate food supply available for mussel (Mytilus spp.) farming in a semi-enclosed northern inlet. Estuarine Coastal Shelf Sci. 53, 107–121.

Platt, T., Gallegos, C.G., Harrison, W.G., 1980. Photoinhibition of photosynthesis in natural assembalges of marine phytoplankton. J. Mar. Res. 38, 687–701.

Platt, T., Jassby, A.D., 1976. The relationship between photosynthesis and light for natural assemblages of coastal marine phytoplankton. J. Phycol. 12, 421–430.

Press, W.H., Teukolsky, S.A., Vetterling, W.T., Flannery, B.P., 1996. Numerical Recipes in Fortran 90. Cambridge University Press, Cambridge 576.

Raillard, O., Ménesguen, A., 1994. An ecosystem box model for estimating the carrying capacity of a macrotidal shellfish ecosystem. Mar. Ecol. Process Ser. 115, 117–130.

Riley, G.A., 1947. A theoretical analysis of the zooplankton population on Georges Bank. J. Mar. Res. 6, 104–113.

Seed, R., 2000. Mussels: space monopolisers or ecosystem engineers. J. Shellfish Res. 19, 611–612.

Soetaert, K., Middelburg, J.J., Herman, P.M.J., Buis, K., 2000. On the coupling of benthic and pelagic biogeochemical models. Earth Sci. Rev. 51, 173–201.

Solidoro, C., Melaku Canu, D., Rossi, R., 2003. Ecological and economic considerations on fishing and rearing of Tapes phillipinarum in the lagoon of Venice. Ecol. Modell. 170, 303–318.

Solidoro, C., Pastres, R., Melaku Canu, D., Pellizzato, M., Rossi, R., 2000. Modelling the growth of Tapes philippinarum in northern Adriatic lagoons. Mar. Ecol. Prog. Ser. 199, 137–148.

Steele, J.H., Henderson, E.W., 1981. A simple plankton model. Am. Nat. 117, 676–691.

Stone, L., Grbric, A., Berman, T., 1996. Ecosystem resilience, stability and productivity: seeking a relationship. Am. Nat. 108, 892–903.

Takeoka, H., 1984. Fundamental concepts of exchange and transport time scales in a coastal sea. Continental Shelf Res. 3, 311–326.

Thompson, K.R., Dowd, M., Shen, Y., Greenberg, D.A., 2002. Probabilistic characterization of mixing in a coastal embayment: A Markov chain approach. Continental Shelf Res. 22, 1063–1614.

Ulanowicz, R.E., Tuttle, J.H., 1992. The trophic consequences of oyster stock rehabilitation in Chesapeake Bay. Estuaries 15, 298–306.

Vallino, J.J., 2000. Improving marine ecosystem models: use of data assimilation and mesocosm experiments. J. Mar. Res. 58, 117–164.

Waniek, J.J., 2003. The role of physical forcing in initiation of spring blooms in the northeast Atlantic. J. Mar. Syst. 39, 57–82.

Widdows, J., Brinsley, M.D., Salkeld, P.N., Elliott, M., 1998. Use of annular flumes to determine the influence of current velocity and bivalves on material flux at the sediment–water interface. Estuaries 21, 552–559.

Wu, J., Marceau, D., 2002. Modelling complex ecological systems: an introduction. Ecol. Modell. 153, 1–6.